NEA/NSC/DOC(95)03/IV
Volume IV

LEU-COMP-THERM-001

WATER-MODERATED U(2.35)O_2 FUEL RODS IN 2.032-CM SQUARE-PITCHED ARRAYS

Evaluator

Virginia F. Dean
Idaho National Engineering Laboratory

Internal Reviewer
Carol A. Atkinson

Independent Reviewer

Nigel R. Smith
AEA Technology

ACKNOWLEDGMENTS

The author wishes to thank three of the experimenters, Sid Bierman, Duane Clayton, and Michael Durst, who provided much valuable additional information about how the experiments were conducted and reviewed the draft evaluation. She would also like to thank Roger Meade and Linda Sandoval of the Los Alamos National Laboratory Archives, who assisted in finding stored logbooks.

WATER-MODERATED U(2.35)O_2 FUEL RODS IN 2.032-CM SQUARE-PITCHED ARRAYS

IDENTIFICATION NUMBER: LEU-COMP-THERM-001 SPECTRA

KEY WORDS: low enriched fuel rods, low enriched uranium, PNL, ^{235}U, uranium dioxide

1.0 DETAILED DESCRIPTION

1.1 Overview of Experiment

A series of critical approach experiments with clusters of aluminum clad U(2.35)O_2 fuel rods in a large water-filled tank was performed over the course of several years at the Critical Mass Laboratory at the Pacific Northwest Laboratories (PNL). Experiments included rectangular, square-pitched lattice clusters, with pitches of 2.032 cm or 1.684 cm. Gadolinium impurity in the water was reported for some experiments (LEU-COMP-THERM-003). Some of these experiments were performed with absorber plates of various materials between clusters (LEU-COMP-THERM-016). Others added reflecting walls of depleted uranium, lead, and steel on two opposite sides of the cluster array (LEU-COMP-THERM-017). Some circular, triangular-pitched lattices, with pitches of 1.598 cm or 1.895 cm, were used to measure the effect of gadolinium dissolved in the water (LEU-COMP-THERM-005).

This evaluation documents water-reflected clusters at 2.032 cm square pitch with no absorber plates, reflecting walls, dissolved poison, or gadolinium impurity. A total of 8 experiments were evaluated. All of these were judged to be acceptable as benchmark data.

Information in this section comes from References 1 - 10, which are the original PNL reports of these experiments. Primary references for these 8 experiments are References 1 and 3. References 11 - 15 provide supplementary information. Details which are from specific references are so noted.

1.2 Description of Experimental Configuration

1.2.1 Experiment Tank and Surroundings - Experiments were performed in a 0.952-cm-thick, open-top, carbon-steel tank. Tank inside dimensions were 1.8 x 3.0 x 2.1 meters deep. The experiment was centered in the tank to within one-quarter inch. The control blade, the safety blade, and any control or safety rods were withdrawn

above the top water reflector for the reported configurations. Other than radiation detectors and support structures (acrylic support plate, acrylic or polyethylene lattice plates, 6061 aluminum angle supports, and control/safety blade guides are described in this section), no other apparatus was in the tank.[a] (See Figures 1 and 2.)

[a] Tank dimensions were from References 1-10. Other information was from private communication, Sid Bierman, July 1993.

Figure 1. Experiment Tank.

Figure 2. Arranging Fuel Rods.

The experiment tank was located in one corner of the Critical Mass Laboratory at the Pacific Northwest Laboratories, Hanford, Washington. The tank sat upon a concrete floor, which was at least 40.6 cm thick (Reference 11, p. 32). The concrete walls of the room were 5 feet thick. The concrete ceiling was 2 feet thick and approximately 20 feet high. The tank was located approximately four feet from the two closest corner walls.[a]

1.2.2 Fuel Rod Support Plate - The bottoms of the fuel rods were supported by a 2.54-cm-thick, acrylic support plate. The width and length of the support plate were approximately the width and length of the clusters. The acrylic support plate

[a] Sid Bierman, private communication, July 1993.

was supported by two 15.3 x 5.08 x 0.635 cm 6061 aluminum channels oriented so that the bottom surface of the support plate was 15.3 cm above the bottom of the tank.[a]

1.2.3 Lattice Plates and Supports - The pitch of the fuel rods was maintained by two levels of acrylic lattice plates. Holes for the fuel rods were no more than 5 mils (0.0127 cm) larger than the rod diameter.[b]

The top lattice plates were bolted to 5.08 x 5.08 x 0.635 cm aluminum angles, attached at their ends to the walls of the tank. In one experiment, these aluminum lattice supports were doubled, with no effect on the critical separation between clusters (Reference 1, pp. 26 and 28).

For 3-cluster experiments from Reference 1 (Cases 2-7), the lattice plates were positioned by twelve 1.27-cm-diameter, vertical aluminum spacer rods at the corners of the lattice plates. The spacer rods were 83.9 cm long. The bottom set of lattice plates was raised approximately 5 or 6 inches above the fuel rod support plate by pieces of Tygon tubing placed on four or five fuel rods in each cluster.[c] In experiments from Reference 3 (a second instance of Case 3 and Case 8), the bottom lattice plates rested on the fuel rod support plate.

A summary of the vertical positions of the lattice plates is given in Table 1. The plates were 1.27 cm thick.

Table 1. Positions of Lattice Plates.

Experiments	Height of bottom surface above fuel rod support plate
Cases 1-7 (Reference 1)	Bottom plate:~14 cm(a) Top plate: ~77 cm(b)
Cases 3, 8 (Reference 3)	Bottom plate: 0 cm Top plate: ~77 cm(b)

(a) Sid Bierman, private communication, August 1993.
(b) Estimated from Figures 2 and 3 in Reference 1, pp. 4 and 6.

[a] Sid Bierman recalls that there may have been three separate support plates for the 3-cluster experiments. Exact dimensions of the support plates are not known. (Private communication, Sid Bierman, August 1993.)

[b] Sid Bierman, private communication, August 1993.

[c] Sid Bierman, private communication, August 1993.

In some 3-cluster experiments, the required horizontal separation between bottom lattice plates or between bottom lattice plates and the control/safety blade guides was maintained by shims. This was necessary in order to position the bottom lattice plates accurately. (The control and safety blade guides could not, by themselves, be used for positioning since they were not fastened to anything below their attachment to the angles supporting the top lattice plates.) The shim was either Lucite or was made from the lattice plate material. The Lucite shim was approximately 1 inch thick.[a]

1.2.4 Radiation Detectors - The boron-lined proportional counters (usually three in number) were placed symmetrically around the experiments. The detectors were kept dry by being placed in aluminum tubes that extended above the top surface of the water. The elevation of the detectors varied, depending on the buoyancy of the tube holding the detector. The aluminum tubes were approximately 1.5 inches in diameter and were placed about 30 cm from the experimental assembly, always outside a 15-cm thickness of water.[b]

1.2.5 Water Reflector - The top water surface was always at least 15 cm above the top of the fuel region of the rods. (Reference 14, p. 132)[c] The bottom water reflector also was at least 15 centimeters thick, since the aluminum angle supporting the fuel-rod support plate above the bottom of the tank was 15.3 cm high. The minimum side-reflector thickness, assuming that the experiment was centered in the tank and that the longer side of the experiment parallelled the longer side of the tank, was approximately 70 cm.[d]

1.2.6 Others - A ^{252}Cf source of approximately 0.6 micrograms was placed near the center of each experimental assembly. The source was mounted in an open acrylic tube, 0.6 cm in diameter (Reference 8, p. 2.3) and two or three inches long.[e] During the triangular-pitched experiments, no measurable effect on critical size was detected with replacement-type reactivity worth measurements of the californium source (Reference 8, pp. 3.6 and 3.7).

The aluminum control and safety blade guides were located between clusters in multi-cluster experiments. The blade guides, two for the control blade and two for the safety blade, extended from the bottom of the fuel pin array to well above the water surface. Two slightly different sizes of guides were used throughout the

---

[a] Private communication, Sid Bierman, August 1993.

[b] Private communication, Sid Bierman, July 1993.

[c] Confirmed by private communication, Sid Bierman, July 1994.

[d] Case 1. See Figure 5.

[e] Private communication, Sid Bierman, August 1993.

series of experiments. For this set of experiments, guides were 3.8 cm wide and 2.54 cm thick (Reference 3, p. 5) with a slot for the blades that was 0.96 cm wide.[a] During one experiment from the first set of experiments, an extra thickness of aluminum was added to the control and safety blade guides. The results demonstrated "no change in the predicted critical separation between fuel rod clusters." (Reference 1, pp. 13 and 28)

1.2.7 Fuel Rods - Fuel rod dimensions are given in diagrams in References 1, 3-6, and 8. These diagrams are the same as Figure 3, which is a reproduction of an annotated diagram from Reference 13 (Vol 1, p. 29). Reference 13 is cited by Reference 8, p. 2.7, as the source of fuel rod data.

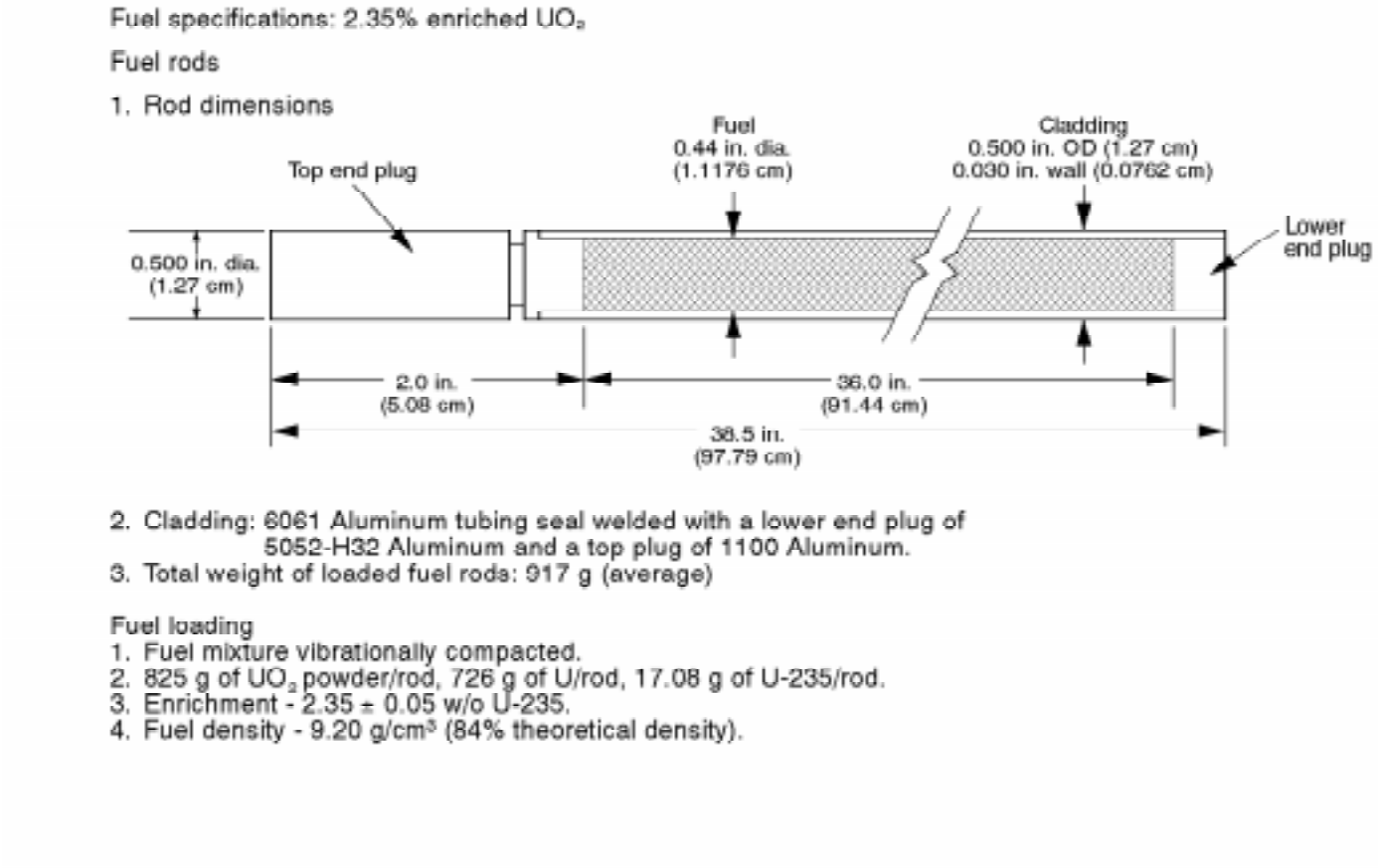

Figure 3. U(2.35)O_2 Fuel Rod.

[a] Different widths of control and safety blades were used for different experiments. (Private communication, Sid Bierman, August 1993.)

Dimensions of the U(2.35)O_2 fuel rods are summarized in Table 2.

Table 2. 2.35 Wt.% Enriched UO_2 Fuel Rod Dimensions.

Component	Length (cm)	Diameter (cm)
UO_2 fuel	91.44	1.1176
Top end plug (1100 Al)	5.080	1.27
Lower end plug (5052-H32 Al)	1.27	1.1176
Clad (6061 Al)	~93.19[(a)]	1.270 OD (.0762 cm thick)

(a) This length is an approximation based on measuring Figure B-1 in Reference 13 (Vol 1, p. 29). Total rod length is 97.79 cm. The clad envelops the lower end plug, fuel, and ~0.48 cm of the top end plug. Dimensions of the notch shown in the top end plug are not known.

1.2.8 Experimental Method for Determining Critical Configuration[a] - The critical configuration was determined by measuring neutron detector count rates (above background) produced by subcritical configurations and extrapolating to the critical condition. In particular, the averages of several (usually four, five, or six) 80-second counts from each of two or three detectors were recorded for at least two loading configurations. For single cluster experiments or those with clusters positioned at predetermined separation distances, a plot of [number of fuel rods]/[count rate] vs. [number of fuel rods] was linearly extrapolated to zero to determine the critical number of rods predicted by each detector. Then the results from the two or three detectors were averaged. Additionally, a plot of [1]/[count rate] vs. [number of fuel rods] was extrapolated to zero for each detector and the results averaged. Then the average critical number of fuel rods from these two averages was used as the final result.

For multiple clusters of predetermined sizes with varying separation distance between them, the same procedure was followed except that the variables plotted were [separation distance]/[count rate] vs. [cluster separation] and [1]/[count

[a] This information is from study of the logbooks, which are stored at the Los Alamos National Laboratory Archives. See Appendix B for correlation between case number in this evaluation and experiment number under which experiment is stored at the archives.

rate] vs. [cluster separation]. The final result was the average cluster separation distance.[a]

To vary the number of fuel rods or cluster separation, fuel rods were moved in half-row or whole-row increments. An example of half-row increment moves for varying cluster separation is shown in Figure 4 for three 15-by-8-rod clusters. For the four configurations represented in this example, the numbers of empty rows between clusters are 2, 1¾, 1½, and 1¼. The initial configuration is shaded. The separation distance resulting from each of the three moves is determined by multiplying the number of empty rows between clusters by the pitch and adding the constant separation distance between lattice plates, required for the control and safety blade guides.[b]

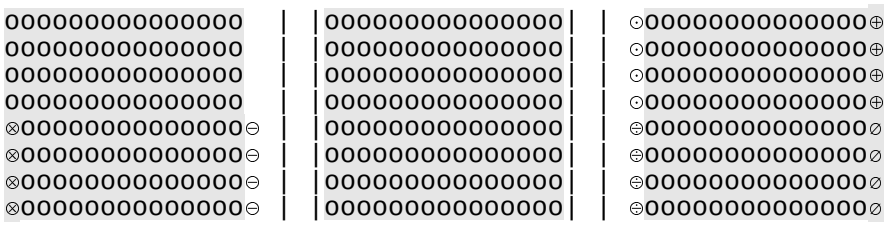

| | are safety and control blade guide widths
Initial load is shaded.

(a) This refers to the resulting average rows of separation between lateral clusters and central cluster after the stated move. Separation distance is then {[average rows of separation] x [pitch]} + [width of safety and control blade guides].

Figure 4. Method of Varying Separation Distances Between Clusters.

[a] Plots of both [number of rods]/[count rate] vs. [number of rods] and [1]/[count rate] vs. [number of rods] (or [separation]/[count rate] vs. [separation] and 1/[count rate] vs. [separation]) were used because one tended to overestimate the critical number of rods and the other to underestimate it. The lower critical number prediction was used in applying the operational safety rule that no more than 85% of the difference between latest loading and predicted critical loading could be added. As criticality was approached, both curves tended to predict the same critical number of rods. (Private communication, Duane Clayton, August 1993.)

[b] Rod additions were in half- or whole-row increments, so that the average rod worth of the addition was equal to the average rod worth of an entire row. Then, in computational models that homogenize the fuel rod cell, partial rows can be represented as a fraction of a fuel rod across the entire width of the cluster.

1.2.9 Critical Cluster Dimensions and Separations - Cluster sizes and separations for the 8 critical configurations are listed in Table 3 and are diagramed in Figure 5. Because the critical configuration was determined by extrapolation to critical, the critical number of rods was not an integral number for the single-cluster case, Case 1.

Table 3. $U(2.35)O_2$ Fuel Rod Critical Configurations. (See Figure 5.)

Case Number	Number of Clusters	Cluster Dimensions (number of rods)[a] (X x Y)	Separation Between Clusters (cm)[b]	Reference (pg)
1	1	20 x 18.08	-	1 (13)
2	3	20 x 17	11.92 ± .04	1 (13)
3	3	20 x 16	8.41[c][d] ± .05	1 (13), 3 (14)
4	3	20 x 16 (center) 22 x 16 (two outer)	10.05 ± .05	1 (13)
5	3	20 x 15	6.39 ± .05	1 (13)
6	3	20 x 15 (center) 24 x 15 (two outer)	8.01 ± .06	1 (13)
7	3	20 x 14	4.46 ± .10	1 (13)
8	3	19 x 16	7.57[d] ± .04	3 (14)

(a) For three-cluster configurations, the first dimension is along the direction of cluster placement. Second dimension is the width of facing sides, as shown in Figure 5.
(b) Distance between outer fuel-rod cell boundaries of clusters.
(c) Average of four values: 8.39, 8.41, 8.42, and 8.44 cm ± 0.05 cm.
(d) Reported separations between clusters for this experiment were rod-surface-to-rod-surface (Sid Bierman, private communication, July 1993). However, the reported separations are actually separations between edges of the holes of the lattice plates (Sid Bierman, private communication, February 1994). The diameter of the holes was slightly larger than the fuel rod diameter, so that the hole-edge-to-hole-edge separation is 0.74 cm rather than 0.762 cm, which is the average rod-surface-to-rod-surface separation (0.762 cm = pitch – rod diameter). Therefore, the cell boundary separations are 0.74 cm less than the separations reported in Reference 3 for the 2.032-cm pitch experiments. This is indicated by footnote (g) of Table II, p. 14, Reference 3, which compares table values to previous experimental results from Reference 1.

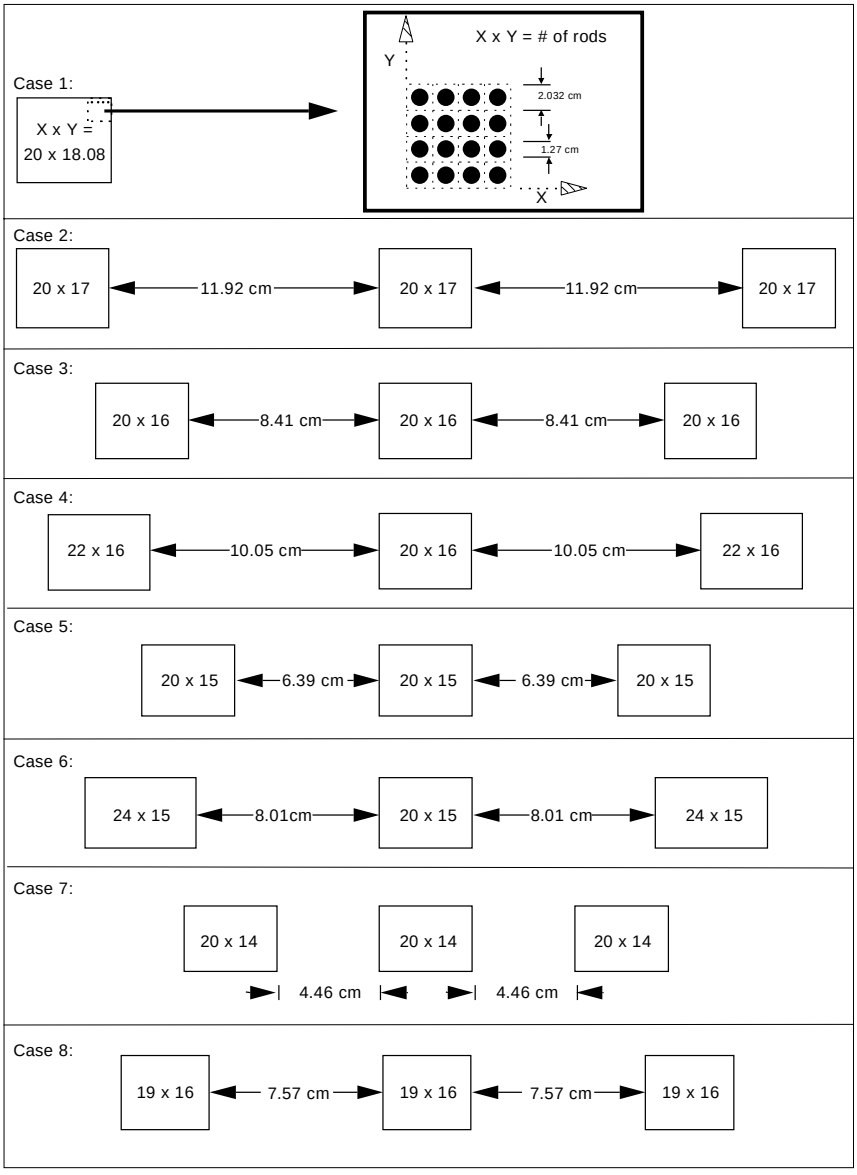

Figure 5. Arrangement of Fuel Rod Clusters for Critical Configuraions of $U(2.35)O_2$ Fuel Rods at 2.032 Centimeter Pitch.

1.3 Description of Material Data

1.3.1 UO_2 Fuel - Figure 3 (from Reference 13, Vol. 1, p. 29) and results of a fuel rod sample analysis (Reference 13, Vol. 2, p. 3) are the basis for the fuel material characterization. A fuel rod contains 825 g of UO_2 powder, 726 g of 2.35 wt.% enriched uranium, and 17.08 g of ^{235}U, at an oxide density of 9.20 g/cm^3.[a] The isotopic content of the uranium is given in Table 4.

Table 4. Isotopic Composition of Uranium in 2.35% Enriched UO_2 Fuel Rods (Reference 8, pp. 2.7 and 2.8).

Uranium Isotope	Wt.%[(a)]
U-234	0.0137 ± .0007
U-235	2.350 ± .01
U-236	0.0171 ± .0007
U-238	97.62

(a) Values are originally from Reference 13, Vol 2, p. 3. Uncertainties are 3σ. Note that the total of all weight percents is 100.008.

1.3.2 Aluminum Alloys - Aluminum components of the fuel rods are the top (longer) end plug of 1100 aluminum, the lower end plug of 5052 aluminum, and the clad of 6061 aluminum. Measured densities and ASTM Standard chemical compositions of these three types of aluminum are given in Table 5.[b] The ASTM Standard for these three aluminum alloys includes limits on impurities to maximums of 0.05 wt.% each and 0.15 wt.% total.

Experiment support structures, including lattice plate supports and spacer rods, control/safety blade guides, tubes housing the proportional counters, and sleeves for gadolinium control rods, were 6061 aluminum alloy. The experimenters noted that doubling the amount of the aluminum angles supporting the grid plates in one experiment (Reference 1, p. 26) and the control and safety blade guides in another (Reference 1, p. 13) "resulted in no change in the predicted critical separation between fuel rod clusters." (Reference 1, p. 28)

[a] These values are not self-consistent. See discussion in Section 2.1.

[b] From Reference 8, pp. A.2-A.4, and from *Alcoa Aluminum Handbook*, Aluminum Company of America, pp. 46-50, 1967.

Table 5. Measured Densities and Standard Compositions of Aluminum Alloys.

Element	Wt.%
1100 Aluminum (density - 2.70 g/cm^3)	
Si	1.0 (combined maximum)
Fe	
Cu	0.05-0.20 (0.12 nominal)
Mn	0.05 (maximum)
Zn	0.10 (maximum)
Al	99.00 (minimum)
5052 Aluminum (density - 2.69 g/cm^3)	
Si	0.45 (combined maximum)
Fe	
Cu	0.10 (maximum)
Mn	0.10 (maximum)
Mg	2.2-2.8 (2.5 nominal)
Cr	0.15-0.35 (0.25 nominal)
Zn	0.10 (maximum)
Al	remainder (96.10-97.65)
6061 Aluminum (density - 2.69 g/cm^3)	
Si	0.40-0.80 (0.6 nominal)
Fe	0.7 (maximum)
Cu	0.15-0.40 (0.25 nominal)
Mn	0.15 (maximum)
Mg	0.8-1.2 (1.0 nominal)
Cr	0.04-0.35 (0.2 nominal)
Zn	0.25 (maximum)
Ti	0.15 (maximum)
Al	remainder (96.00-98.61)

1.3.3 Water - Laboratory analyses of the water in the tank were done. The reported impurity concentrations are given in Table C.1 of Appendix C. The approximate

average water temperature was 22°C.[a] This corresponds to a density of 0.997766 g/cm^3.[b]

1.3.4 Lattice Plates and Fuel Rod Support Plates - The acrylic fuel rod support plates and lattice plates had a density of 1.185 g/cm^3 and were 8 wt.% hydrogen, 60 wt.% carbon, and 32 wt.% oxygen. (Reference 4, pp. 11 and 20; Reference 14, p. 133) Uncertainties and methods of determination were not given.

1.3.5 Tank - The experiment tank was carbon steel, which is approximately 1 wt.% Mn, 0.9 wt.% C, and the remainder, 98.1 wt.%, Fe.[c]

[a] Estimated from occasional logbook values.

[b] Interpolated between densities at 20 and 25°C, CRC Handbook of Chemistry and Physics, 68th Edition, p. F-10.

[c] Robert C. Weast, ed., *CRC Handbook of Chemistry and Physics, 68th Edition*, CRC Press, p. E-114, 1987.

2.0 EVALUATION OF EXPERIMENTAL DATA

Experiments were well documented and carefully performed. There were no significant omissions of data.

2.1 Fuel Rod Data

Some uncertainty exists in the characterization of the fuel rods. Dimensions and masses are stated in the source document (Reference 13, Vol. 1, p. 29) with no mention of measurement techniques or uncertainties. The 3σ-uncertainty in enrichment is stated as 0.01 wt.% without further discussion (Reference 13, Vol. 2, p. 3).

As was mentioned in Section 1.3, quantities characterizing the mass of fuel are not self-consistent. Table 6 gives the mass of ^{235}U derived in different ways from the given quantities. The highest and lowest masses represent a difference in uranium mass of less than 0.2% (726 g vs. 727.22 g).

Table 6. Mass of ^{235}U Per U(2.35)O_2 Fuel Rod Derived from Different Sets of Given Quantities.

U-235 mass derived from the following given quantities:	U-235 Mass (g)
U-235 mass[(a)]	17.08
Mass of U (726 g)[(b)] and 2.35 wt.% ^{235}U	17.0610
Mass of UO_2 (825 g)[(c)] and 2.07 wt.% ^{235}U in UO_2 [(d)]	17.0775[(e)]
UO_2 density (9.20 g/cm^3)[(c)], volume of fuel[(f)], and 2.07 wt.% ^{235}U in UO_2 [(d)]	17.0827
Mass of UO_2 (825 g)[(c)], 2.35 wt.% ^{235}U, and 2-to-1 ratio of O atoms to U atoms in UO_2	17.0896
Total rod mass (917 g)[(a)], volume[(f)] and density of aluminum, and 2.07 wt.% ^{235}U in UO_2 [(d)]	17.0775

(a) Given only in Reference 1.
(b) Given in References 1 and 8.
(c) Given in all reports on experiments with 2.35 wt.% enriched rods. (References 1, 3-6, and 8.)
(d) Reference 13, Vol. 2, p. 3.
(e) Using this mass and the given wt.%'s of the uranium isotopes gives a formula for uranium dioxide of $UO_{2.012}$. This is within the typical range for UO_2 powders of $UO_{2.005}$ and $UO_{2.129}$.[a]
(f) Calculated from reported dimensions.

The magnitudes of other uncertainties in fuel rod data are taken as half the value of the least significant digit, when the uncertainty is not given. The effects on k_{eff} of the uncertainties in enrichment, fuel diameter, fuel length, clad thickness, pitch, and uranium mass for a near-critical configuration are summarized in Table 7. The last two entries are the calculated results from two models that contain a combination of individual changes. Results indicate that effects on k_{eff} due to uncertainties in fuel rod characterization and pitch could be

[a] C. R. Tipton, Jr., ed., *Reactor Handbook, Second Edition*, Interscience Publishers, Inc., N.Y., Vol. I, p. 292.

as great as 0.30%. Note that this is for the case of all rods having all changes that affect k_{eff} positively, which is unlikely. Also, the uncertainty in pitch is itself especially conservative, (See footnote c of Table 7.) However, an uncertainty of ± 0.30% due to uncertainties in fuel rod characterization may be included in the benchmark-model k_{eff}.

Table 7. Sensitivity of k_{eff} to Uncertainties in Fuel Rod Characterization.

Quantity (Amount of Change)	% Δk_{eff} (ONEDANT)[a] for Increase in the Quantity	% Δk_{eff} (ONEDANT)[a] for Decrease in the Quantity
Enrichment (± 0.01 wt.%[b])	+0.10	-0.09
Fuel Diameter (± 0.0127 cm)	+0.10	-0.08
Fuel Length (± 0.127 cm)	-0.07	0.00
Clad Diameter (± 0.00127 cm)	-0.00	+0.01
Pitch (± 0.0076 cm[c])	-0.14	+0.21
Uranium Mass (-0.81 g and +0.41 g)	+0.03	+0.01
All above changes that individually increase k_{eff}	Δk_{eff} = +0.30%	
All above changes that individually decrease k_{eff}	Δk_{eff} = -0.29%	

(a) 27-group cross sections with homogenized lattice-cell fuel region (CSASIX); sample input given in Appendix D.
(b) 3σ uncertainty (Reference 13, Vol. 2, p. 3)
(c) The largest standard deviation for sets of center-to-center spacing measurements for triangular pitch lattice plates of Reference 8 (Appendix E) was 0.003 inch (0.0076 cm). References 7 (p. 2) and 8 (p. 36) give the uncertainty in pitch as ± 0.005 cm. References 9 (p. 3.2) and 10 (Appendix D) give the uncertainty in pitch as ± 0.001 cm.

2.2 Reflector Thickness

2.2.1 Top Water Reflector - The minimum thickness of the top water reflector is 15 cm above the fuel region. Since the top end plug is 2 inches (5.08 cm) long, the minimum water reflector thickness above the rods is 9.92 cm.

Calculations were performed for an infinite-slab fuel region with a water reflector on both sides. ONEDANT and 27-group cross sections, with a lattice-cell fuel region homogenized by XSDRNPM, were used. The reflector thickness was varied from 15 to 30 centimeters. The effect on k_{eff} of the outermost 15 centimeters of

water was less than 0.002%. Replacing the outermost 15 centimeters of water with 40 centimeters of full-density stainless steel or concrete gave similar results: the effect on k_{eff} was less than 0.004%.

These calculations indicate that a top water reflector with a thickness of 15 centimeters may be considered as "effectively infinite" and the effects of materials beyond the top and bottom reflectors may be neglected. Therefore, the lack of data about material above the 15-cm-thick top water reflector does not affect the acceptability of these experiments as benchmark critical experiments.

2.2.2 Side Water Reflector - Additionally, ONEDANT was used to determine the effect of radial-reflector thickness for a near-critical, cylindrical, XSDRN-homogenized array of pins. The difference in k_{eff} between a 15-cm-thick side reflector and a 30-cm-thick side reflector is 0.01%. Replacing the outermost 15 centimeters of the 30-cm-thick water reflector with 20% stainless steel in water affects k_{eff} by less than 0.002%. Therefore, lack of specifications about detectors, which were placed in the water reflector more than 15 centimeters away from the clusters, does not affect the acceptability of these experiments.

2.3 Water Impurities

Water impurity sensitivity studies in Appendix C, discussed in Section 3.3.2, indicate that none of the reported water impurities in References 1 and 3 have a significant effect on k_{eff}.

2.4 Temperature Data

Water temperatures were recorded in logbooks for approximately ten percent of the experiments. Measured temperatures ranged from 18°C to 26°C. ONEDANT calculations with 27-group cross sections, for an infinite slab of fuel pins reflected on both sides by 15 cm of water gave a change in k_{eff} of 0.01% between these two extremes of temperature. Therefore, an estimate of the uncertainty in k_{eff} due to the effects of temperature is half of this amount, namely 0.005%.

2.5 Cluster Separations

The measurement uncertainties in cluster separation (See Table 3.) vary from 0.04 cm to 0.10 cm. To estimate the effect on k_{eff} of this uncertainty, cluster separations were reduced for Cases 2 - 8 and calculated, using KENO V.a with 27-group ENDF/B-IV cross sections. The average Δk_{eff} per 0.01 cm reduction in separation was 0.009%.

The uncertainties to be included in the benchmark-model k_{eff} due to uncertainty in the cluster separation measurement are listed in Table 8. Case 1 is not listed because it was a single-cluster configuration.

Table 8. Uncertainties in Benchmark-Model k_{eff} Due to Cluster Separation Measurement Uncertainty.

Case Number	Uncertainty in Separation Measurement (cm)	Δk_{eff}(%) to Include in Uncertainty of Benchmark-Model k_{eff}
2	0.04	0.04
3 - 5	0.05	0.05
6	0.06	0.05
7	0.10	0.09
8	0.04	0.04

3.0 BENCHMARK SPECIFICATIONS

3.1 Description of Model

The calculational models consist of square-pitched, aluminum-clad cylindrical fuel pins in water arranged in rectangular clusters. Descriptions of the critical configurations, including cluster dimensions, separations, and fuel rod pitch, are given in Table 3 and are shown in Figure 5.

3.2 Dimensions

Fuel rod dimensions, as modelled, are shown in Figure 6. The entire rod has a diameter of 1.27 cm and is 97.79 cm long. The UO_2 fuel region has a diameter of 1.1176 cm and is 91.44 cm long. The clad is 0.0762 cm thick and 93.19 cm long. The clad surrounds the fuel, the lower end plug, and 0.48 cm of the top end plug. There is no gap between the clad and fuel or end plugs. The top end plug is 5.08 cm long. The lower end plug is 1.27 cm long.

The bottom reflector is a single 2.54-cm-thick acrylic plate, which extends horizontally to the outermost cell-boundary edges of the clusters, followed by 15.3 cm of water. The four side reflectors are 30-cm-thick water. The top reflector is 9.92 cm of water.

Configurations are described in Table 3 and Figure 5. The model of Case 1 is a 20 x 18 array of fuel rods with a 19^{th} row containing 1 fuel rod at the end of the row.

3.3 Material Data

3.3.1 Fuel Rods - The fuel region consists of 825 g of UO_2. The mass of ^{235}U in each rod is 17.08 g. The isotopic composition of the uranium is 0.0137 wt.% ^{234}U, 2.35 wt.% ^{235}U, 0.0171 wt.% ^{236}U, and 97.6192 wt.% ^{238}U.[a]

Fuel rods have 6061 aluminum clad, with a 5052 aluminum lower end plug and a 1100 aluminum top end plug, as shown in Figure 6. Aluminum clad and end-plug components are nominal, mid-range, half-maximum, or minimum values, totalling 100 wt.%, as given in Table 5. Atom densities are given in Table 9.

[a] This is slightly less than the wt.% for ^{238}U of 97.62 quoted in Section 1, in order that all weight percents add to 100. It is inferred from a footnote to Table I, Reference 13, vol. 2, p. 3, that the wt.% of ^{238}U is the balance. Therefore, the ^{238}U wt.% of the benchmark model is determined by balance.

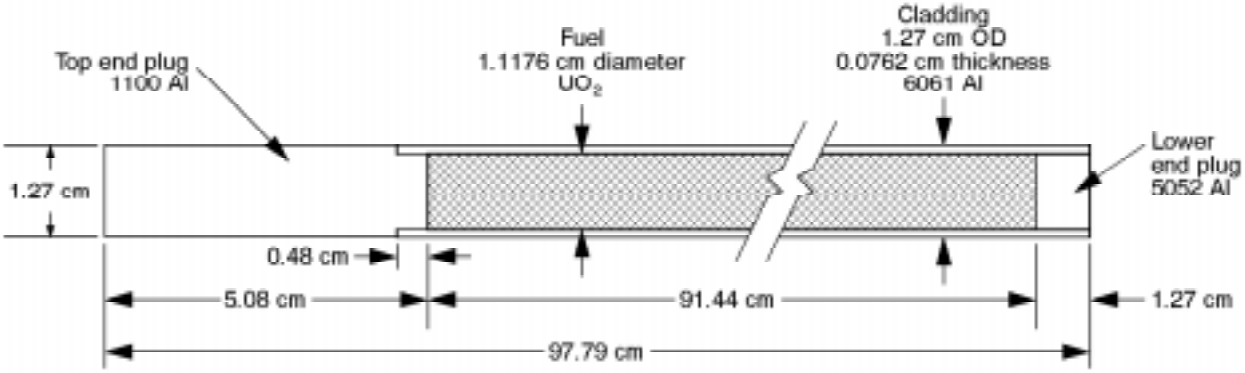

Figure 6. Fuel Rod Model.

Table 9. Fuel Rod Atom Densities.

Material	Isotope	Wt.%	Atom Density $(barn\text{-}cm)^{-1}$
$U(2.35)O_2$ fuel	^{234}U	0.0137	2.8563×10^{-6}
	^{235}U	2.35	4.8785×10^{-4}
	^{236}U	0.0171	3.5348×10^{-6}
	^{238}U	97.62	2.0009×10^{-2}
	O	-	4.1202×10^{-2}
1100 Aluminum (top end plug; 2.70 g/cm^3)	Al	99.0	5.9660×10^{-2}
	Cu	.12	3.0705×10^{-5}
	Mn	.025	7.3991×10^{-6}
	Zn	.05	1.2433×10^{-5}
	Si	.4025	2.3302×10^{-4}
	Fe	.4025	1.1719×10^{-4}
5052 Aluminum (lower end plug; 2.69 g/cm^3)	Al	96.65	5.8028×10^{-2}
	Cr	.25	7.7888×10^{-5}
	Cu	.05	1.2746×10^{-5}
	Mg	2.5	1.6663×10^{-3}
	Mn	.05	1.4743×10^{-5}
	Zn	.05	1.2387×10^{-5}
	Si	.225	1.2978×10^{-4}
	Fe	.225	6.5265×10^{-5}
6061 Aluminum (clad; 2.69 g/cm^3)	Al	97.325	5.8433×10^{-2}
	Cr	.2	6.2310×10^{-5}
	Cu	.25	6.3731×10^{-5}
	Mg	1.0	6.6651×10^{-4}
	Mn	.075	2.2115×10^{-5}
	Ti	.075	2.5375×10^{-5}
	Zn	.125	3.0967×10^{-5}
	Si	.6	3.4607×10^{-4}
	Fe	.35	1.0152×10^{-4}

Sensitivity Studies. In order to test the sensitivity of the critical configurations to the small amounts of alloying substances in the aluminum, a near-critical, cylindrical, water-reflected lattice of rods at pitch 2.032 cm was used. The thickness of the clad was increased so that the clad volume was equal to the volume of the actual clad plus the two end plugs, so that this calculation is a conservative estimate of the effects of varying the clad composition.

Four cases were calculated with ONEDANT. Clad for the four cases were each of the three alloys plus pure aluminum. Results are given in Table 10. The greatest change in k_{eff} is 0.17% when pure aluminum clad is used. Therefore, to more accurately represent the fuel rods for this benchmark, nominal amounts of all constituents are included in the specified aluminum alloys.

Table 10. Results of ONEDANT Calculations of k_{eff} for Cylindrical Arrangements of $U(2.35)O_2$ Fuel Rods with Different Aluminum Claddings.[(a)]

Clad Material (thickness increased from 0.07620 cm to 0.09788 cm)	Δk_{eff} (%, ONEDANT)
6061 aluminum[(b)]	-
1100 aluminum[(b)]	0.04
5052 aluminum[(b)]	0.12
aluminum[(c)]	0.17

(a) 27-group homogenized fuel-rod mixture cross sections created by CSASIX.
(b) Alloys contain minimum amounts of aluminum and maximum amounts of other components (See Tables 5 and 11.).
(c) Density is nominal ^{27}Al density of 6061 aluminum alloy (97.325 wt.% of 2.69 g/cm^3).

3.3.2 Moderator-Reflector - Fuel rods rest on an acrylic support plate, with a density of 1.185 g/cm^3 and a composition of 8 wt.% hydrogen, 60 wt.% carbon, and 32 wt.% oxygen. The moderator-reflector is water at a temperature of 22°C. Atom densities are given in Table 11.

Table 11. Moderator-Reflector Atom Densities.

Material	Isotope	Atom Density $(barn\text{-}cm)^{-1}$
Water[(a)]	H	6.6706×10^{-2}
	O	3.3353×10^{-2}
Acrylic	H	5.6642×10^{-2}
	C	3.5648×10^{-2}
	O	1.4273×10^{-2}

(a) This is 0.997766 g/cm^3, interpolated from densities at 20 and 25°C. (CRC Handbook of Chemistry and Physics, 68th edition, p F-10.)

Sensitivity Studies. *Water Impurities*. The effects on k_{eff} of impurities in the water moderator-reflector for a near-critical cylindrical cluster of $U(2.35)O_2$ fuel pins, as calculated by ONEDANT, are given in Appendix C. All impurities except boron and gadolinium affect the calculated value of k_{eff} by less than 0.005%. No boron or gadolinium impurities were recorded for experiments included in this evaluation.

Bottom Reflector. The model of the bottom reflector is 2.54 cm of acrylic followed by 15.3 cm of water. The effects on k_{eff} of the one-inch-thick acrylic support plate directly beneath the fuel rods and the carbon-steel tank 17.84 cm below the fuel rods were calculated using ONEDANT. Results are shown in Table 12. The conclusions are that replacing the carbon steel tank with water has no effect, and replacing the acrylic support plate with water has a small effect (0.05%). Therefore, the support plate is retained in the benchmark model.

Because of the negligible effect of materials beyond the water reflector region (See Section 2.2.), concrete floors and walls are not included in the benchmark model.

Table 12. Calculated Effect[(a)] of Bottom Reflector Materials on k_{eff}.

Reflector			Δk_{eff} (%)
Inner 2.54 cm	Middle 15.3 cm	Outer 0.952 cm	
acrylic	water	carbon steel	-
acrylic	water	water	+0.00
water	water	water	-0.05

(a) ONEDANT slab model with CSAS 27-group cross sections and homogeneous fuel region mixture created by XSDRNPM. Reflector materials are on both sides of an infinite slab of the homogenized fuel-pin mixture.

Lattice Plates. The acrylic lattice plates are omitted from the benchmark model. However, as given in Table 1, Cases 1 - 7 have two acrylic lattice plates at approximately 30 cm above and below the middle of the fuel pins. Case 8 has an upper acrylic lattice plate placed as in Cases 1 - 7 and a lower acrylic lattice plate resting on the acrylic support plate, just below the fuel region.

The effects of the lattice plate resting on the support plate and of a lattice plate approximately 30 cm from the center of the fuel pins were calculated. A ONEDANT slab model with CSAS 27-group cross sections and homogeneous fuel region mixture created by XSDRNPM with a 15-cm-thick water reflector was used. The effect was approximately 0.01% Δk_{eff} for each plate. Therefore, the effect on k_{eff} of lattice plates is 0.02%. Since lattice plates are omitted from the benchmark model, this small positive contribution to k_{eff} may be subtracted from the benchmark-model k_{eff}.

3.4 Temperature Data

Temperature data for the individual experiments were not published.

Logbook records give temperature data for approximately every tenth experiment. Recorded values vary between 18°C and 26°C, with most values between 20°C and 25°C. An approximate temperature of 22°C (295 K) was used in the models.

A sensitivity study of temperature variation (See Section 2.4.) demonstrated that the effects on k_{eff} of temperature were small (less than 0.005% for half of the temperature range). The effect is included in the uncertainty of the benchmark-

model k_{eff}. Therefore, any reasonable approximation to room temperature may be used in the model.

3.5 Experimental and Benchmark-Model k_{eff}

The reported configurations were extrapolations to critical configurations. Therefore, the experimental k_{eff} was 1.000.

Because of calculated effects of acrylic lattice plates which were omitted from the benchmark model, the benchmark-model k_{eff} is slightly below 1.0. The benchmark-model k_{eff} is 0.9998.

Other model simplifications (no aluminum support structures; no reflector beyond 30 cm of water on the sides, 15 cm of water above, and 15.3 cm of water below; no measurement devices in the water, no notch in the top end plug) were judged to have negligible effects on k_{eff}. However, some experimental uncertainties and model simplifications, described in sensitivity studies above, contribute to the estimated uncertainty in the benchmark-model k_{eff}. Those included are listed in Table 13.

Table 13. Uncertainty in Benchmark-Model k_{eff}.

Measurement Uncertainty or Model Simplification	Δk_{eff}	
Fuel rod characterization	0.0030	
Temperature	0.00005	
Cluster Separation	Case 2	0.0004
	Cases 3-6	0.0005
	Case 7	0.0009
	Case 8	0.0004
Total Uncertainty in k_{eff} [(a)]	Cases 1-6, 8	0.0030
	Case 7	0.0031

(a) Square root of sum of squares of individual Δk_{eff} values.

Therefore, the benchmark-model k_{eff} is 0.9998 ± 0.0031.

4.0 RESULTS OF SAMPLE CALCULATIONS

Results of calculations representing the eight critical configurations are presented in Table 14. Code versions and modelling options are discussed briefly in paragraphs preceding the input listings in Appendix A.

All results are below the benchmark-model k_{eff} of 0.9998. All except one of the KENO results are below the range of k_{eff} that includes the estimated uncertainty (below 0.9967); more than half are low by 0.5-1%. Of the three MCNP results that are below the uncertainty range, only one is more than 0.5% below the benchmark-model k_{eff}. (Case 8 is 0.8% low.) Therefore, k_{eff} is underpredicted slightly for all three codes.[a]

Table 14. Sample Calculation Results (United States).

Code (Cross Sections Set)→ Case Number ↓	KENO (Hansen-Roach)[(a)]	KENO (27-Group ENDF/B-IV)	MCNP (Continuous Energy ENDF/B-V)
1	0.9921 ± .0017	0.9914 ± .0011	0.9987 ± .0016
2	0.9960 ± .0016	0.9904 ± .0016	0.9977 ± .0017
3	0.9958 ± .0018	0.9888 ± .0016	0.9956 ± .0016
4	0.9943 ± .0016	0.9962 ± .0016	0.9992 ± .0014
5	0.9974 ± .0018	0.9890 ± .0017	0.9970 ± .0016
6	0.9921 ± .0017	0.9931 ± .0015	0.9955 ± .0015
7	0.9930 ± .0015	0.9919 ± .0017	0.9968 ± .0017
8	0.9922 ± .0016	0.9906 ± .0016	0.9921 ± .0015

(a) Cross sections were the original Hansen-Roach 16-group set, except for the following: ^{234}U and ^{236}U (Mihalczo Mod of H-R U-238); Cr (AEROJET); Cu, Mg, Mn, Si (XSDRN); Ti and Zn (GAM-2).

[a] According to W. Rothenstein, "Thermal-Reactor Lattice Analysis Using ENDF/B-IV Data with Monte Carlo Resonance Reaction Rates," Nuclear Science and Engineering, 1976, vol. 59, pp. 337-349, the ENDF/B-IV representation of the low-lying ^{238}U resonances leads to low eigenvalues (by approximately 1%) for water-reflected low-enriched UO_2 lattices.

5.0 REFERENCES

1. S. R. Bierman, E. D. Clayton, and B. M. Durst, "Critical Separation Between Subcritical Clusters of 2.35 Wt% ^{235}U Enriched UO_2 Rods in Water with Fixed Neutron Poisons," PNL-2438, Battelle Pacific Northwest Laboratories, Richland, Washington, October 1977.

2. S. R. Bierman, B. M. Durst, and E. D. Clayton, "Critical Separation Between Subcritical Clusters of 4.29 Wt% ^{235}U Enriched UO_2 Rods in Water with Fixed Neutron Poisons," NUREG/CR-0073, Battelle Pacific Northwest Laboratories, Richland, Washington, May 1978.

3. S. R. Bierman, B. M. Durst, and E. D. Clayton, "Criticality Experiments with Subcritical Clusters of 2.35 Wt% and 4.29 Wt% ^{235}U Enriched UO_2 Rods in Water with Uranium or Lead Reflecting Walls, Near Optimum Water-to-Fuel Volume Ratio," NUREG/CR-0796, Vol. 1, PNL-2827, Battelle Pacific Northwest Laboratories, Richland, Washington, April 1979.

4. S. R. Bierman, and E. D. Clayton, "Criticality Experiments with Subcritical Clusters of 2.35 Wt% and 4.31 Wt% ^{235}U Enriched UO_2 Rods in Water at a Water-to-Fuel Volume Ratio of 1.6," NUREG/CR-1547, PNL-3314, Battelle Pacific Northwest Laboratories, Richland, Washington, July 1980.

5. S. R. Bierman, and E. D. Clayton, "Criticality Experiments with Subcritical Clusters of 2.35 Wt% and 4.31 Wt% ^{235}U Enriched UO_2 Rods in Water with Steel Reflecting Walls," NUREG/CR-1784, PNL-3602, Battelle Pacific Northwest Laboratories, Richland, Washington, April 1981.

6. S. R. Bierman, B. M. Durst, and E. D. Clayton, "Criticality Experiments with Subcritical Clusters of 2.35 Wt% and 4.31 Wt% ^{235}U Enriched UO_2 Rods in Water with Uranium or Lead Reflecting Walls, Undermoderated Water-to-Fuel Volume Ratio of 1.6," NUREG/CR-0796, PNL-3926, Vol. 2, Battelle Pacific Northwest Laboratories, Richland, Washington, December 1981.

7. B. M. Durst, S. R. Bierman, and E. D. Clayton, "Critical Experiments with 4.31 Wt% ^{235}U Enriched UO_2 Rods in Highly Borated Water Lattices," NUREG/CR-2709, PNL-4267, Battelle Pacific Northwest Laboratories, Richland, Washington, August 1982.

8. S. R. Bierman, E. S. Murphy, E. D. Clayton, and R.T. Keay, "Criticality Experiments with Low Enriched UO_2 Fuel Rods in Water Containing Dissolved Gadolinium," PNL-4976, Battelle Pacific Northwest Laboratories, Richland, Washington, February 1984.

9. S. R. Bierman, "Criticality Experiments to Provide Benchmark Data on Neutron Flux Traps," PNL-6205, UC-714, Battelle Pacific Northwest Laboratories, Richland, Washington, June 1988.

10. S. R. Bierman, "Criticality Experiments with Neutron Flux Traps Containing Voids," PNL-7167, TTC-0969, UC-722, Battelle Pacific Northwest Laboratories, Richland, Washington, April 1990.

11. B. M. Durst, S. R. Bierman, E. D. Clayton, J. F. Mincey, and R. T. Primm III, "Summary of Experimental Data for Critical Arrays of Water Moderated Fast Test Reactor Fuel," PNL-3313, ORNL/Sub-81/97731/1, Battelle Pacific Northwest Laboratories, Richland, Washington, May 1981.

12. S. R. Bierman, B. M. Durst, and E. D. Clayton, ""Critical Separation between Subcritical Clusters of Low Enriched UO_2 Rods in Water with Fixed Neutron Poisons," Nuc. Technol., **42**, pp. 237-249, March 1979.

13. R. I. Smith and G. J. Konzek, principal investigators, "Clean Critical Experiment Benchmarks for Plutonium Recycle in LWR's," NP-196, Volumes 1 and 2, Battelle Pacific Northwest Laboratories, Richland, Washington, April, 1976, and September 1978.

14. S. R. Bierman and E .D. Clayton, "Criticality Experiments with Subcritical Clusters of 2.35 and 4.31 wt% ^{235}U-Enriched UO_2 Rods in Water with Steel Reflecting Walls," Nuc. Technol., **54**, August 1981.

15. S. R. Bierman, B. M. Durst, and E. D. Clayton, "Criticality Experiments with Subcritical Clusters of Low Enriched UO_2 Rods in Water with Uranium or Lead Reflecting Walls," Nuc. Technol., **47**, January 1980.

APPENDIX A: TYPICAL INPUT LISTINGS

A.1 KENO Input Listings

The version of KENO V.a used was SCALE 4.0 (creation date: 08/09/91, for standalone KENO V.a with Hansen-Roach Cross Sections, provided by the Radiation Shielding Information Center; creation date: 07/20/92, for KENO V.a with CSAS 27-Group ENDF/B-IV Cross Sections).

KENO V.a input files were created with arrays of fuel rod units. Cuboids of water provided the separation between clusters of rods.

KENO V.a was run using 110 active generations of 1500 neutrons each, after skipping 50 generations, for a total of 165,000 averaged neutron histories. For the 27-group calculation for Case 1, which was also used in sensitivity studies, more neutrons (185,000) were used.

The resonance correction used to determine the Hansen-Roach cross section IDs for ^{235}U and ^{238}U was calculated using the formula

$$\sigma_{pj} = \sum_{i}^{n} \frac{\sigma_{si} N_i}{N_j} + \frac{1-C}{2r_f N_j}$$

σ_{pj} is the resonance correction for the j^{th} fissile nuclide. N_i is the atom density of the i^{th} nuclide in the fuel mixture, n is the number of different nuclides in the fuel mixture, and σ_{si} is the scattering cross section in the resonance region for the i^{th} component of the mixture. Values used for σ_{si} were 12 for uranium and 3.7 for oxygen. Linear interpolation was used to apportion atom densities between the two uranium cross section sets whose σ_p values were closest to the calculated σ_p.

The last term is the Wigner-Rational correction. C is the Dancoff correction factor and r_f is the radius of the cylindrical fuel region of the fuel rod. (The value of C, the Dancoff correction factor, calculated by CSAS, was 0.08602 for 2.032 cm pitch.)

KENO-V.a Input Listing for Case 1 of Table 14 (16-Energy-Group Hansen-Roach Cross Sections).

```
K01  20X18.08 CLUSTER (20X18 + 1 ROD), 2.032 PITCH
READ PARA TME=200 GEN=160 NPG=1500 NSK=50 NUB=YES
LIB=41 XS1=YES RUN=YES LNG=60000    END PARA
READ MIXT  SCT=3 MIX=1
' U(2.35)02
92400 2.8563-6  92509 3.6755-4  92510 1.2030-4
92600 3.5348-6  92858 2.0009-2  8100 4.1202-2
MIX=2
' water
1102 6.6706-2   8100 3.3353-2
MIX=3
' 6061 Al (clad)
13100 5.8433-2  24100 6.2310-5  29100 6.3731-5
12100 6.6651-4  25100 2.2115-5  22100 2.5375-5
30100 3.0967-5  14100 3.4607-4  26100 1.0152-4
MIX=4
'  1100 Al (top end plug)
13100 5.9660-2  29100 3.0705-5  25100 7.3991-6
30100 1.2433-5  14100 2.3302-4  26100 1.1719-4
MIX=5
' 5052 Al (lower end plug)
13100 5.8028-2  24100 7.7888-5  29100 1.2746-5
12100 1.6663-3  25100 1.4743-5  30100 1.2387-5
14100 1.2978-4  26100 6.5265-5
MIX=6
' acrylic
1102 5.6642-2  6100 3.5648-2  8100 1.4273-2
END MIXT
READ GEOM
UNIT 1
 COM=* FUEL PIN *
 CYLINDER  1 1  0.5588 91.44 0.0
 CYLINDER  4 1  0.5588 91.92 0.0
 CYLINDER  5 1  0.5588 91.92 -1.27
 CYLINDER  3 1  0.635  91.92 -1.27
 CYLINDER  4 1  0.635  96.52 -1.27
 CUBOID  2 1  4P1.016 96.52 -1.27
UNIT 2
 COM=* WATER FUEL PIN *
 CUBOID  2 1  4P1.016 96.52 -1.27
UNIT 3
 COM=* 20X18 ARRAY OF FUEL PINS *
 ARRAY 1 3R0
UNIT 4
 COM=* ONE FUEL PIN AT END OF SIDE *
 ARRAY 2 3R0
GLOBAL
UNIT 5
 COM=* 20X18 ARRAY WITH ONE FUEL PIN ADDED AT END OF SIDE *
 ARRAY 3 3R0
 REPLICATE 6 1  5R0.0 2.54  1
 REPLICATE 2 1  4R30.0 9.92 15.3  1
END GEOM
READ ARRAY  ARA=1 NUX=20 NUY=18  FILL F1 END FILL
          ARA=2 NUX=20 NUY=1  FILL  1 19R2  END FILL
          ARA=3 NUX=1 NUY=2  FILL  3 4  END FILL
END ARRAY
END DATA
END
```

KENO-V.a Input Listing for Case 2 of Table 14 (16-Energy-Group Hansen-Roach Cross Sections).

```
K02  CASE 2  THREE 20X17 CLUSTERS, 11.92 CM SEPARATION
READ PARA TME=200 GEN=160 NPG=1500 NSK=50 NUB=YES
LIB=41 XS1=YES RUN=YES LNG=60000    END PARA
READ MIXT  SCT=3
MIX=1
' U(2.35)02
92400 2.8563-6  92509 3.6755-4  92510 1.2030-4
92600 3.5348-6  92858 2.0009-2  8100 4.1202-2
MIX=2
' water
1102 6.6706-2   8100 3.3353-2
MIX=3
' 6061 Al (clad)
13100 5.8433-2  24100 6.2310-5  29100 6.3731-5
12100 6.6651-4  25100 2.2115-5  22100 2.5375-5
30100 3.0967-5  14100 3.4607-4  26100 1.0152-4
MIX=4
'  1100 Al (top end plug)
13100 5.9660-2  29100 3.0705-5  25100 7.3991-6
30100 1.2433-5  14100 2.3302-4  26100 1.1719-4
MIX=5
' 5052 Al (lower end plug)
13100 5.8028-2  24100 7.7888-5  29100 1.2746-5
12100 1.6663-3  25100 1.4743-5  30100 1.2387-5
14100 1.2978-4  26100 6.5265-5
MIX=6
' acrylic
1102 5.6642-2  6100 3.5648-2  8100 1.4273-2
END MIXT
READ GEOM
UNIT 1
 COM=* FUEL PIN *
 CYLINDER  1 1  0.5588 91.44 0.0
 CYLINDER  4 1  0.5588 91.92 0.0
 CYLINDER  5 1  0.5588 91.92 -1.27
 CYLINDER  3 1  0.635  91.92 -1.27
 CYLINDER  4 1  0.635  96.52 -1.27
 CUBOID  2 1  4P1.016 96.52 -1.27
UNIT 2
 COM=* 20X17 ARRAY OF 340 FUEL PINS *
 ARRAY 1 3R0
UNIT 3
 COM=* WATER BETWEEN CLUSTERS, 11.92 CM WIDE *
 CUBOID  2 1  11.92 0.0 34.544 0.0 96.52 -1.27
GLOBAL
UNIT 4
 COM=* ARRAY OF 3 CLUSTERS, 1 IN. ACRYLIC BELOW, WATER REFL *
 ARRAY 2 3R0
 REPLICATE 6 1  5R0.0 2.54  1
 REPLICATE 2 1  4R30.0 9.92 15.3  1
END GEOM

READ ARRAY  ARA=1 NUX=20 NUY=17  FILL F1 END FILL
          ARA=2 NUX=5  FILL 2 3 2 3 2 END FILL
END ARRAY
END DATA
END
```

KENO-V.a Input Listing for Case 4 of Table 14 (16-Energy-Group Hansen-Roach Cross Sections).

```
K04  CASE 4  CENTER 20X16 CLUSTER, TWO 22X16 CLUSTERS, 10.05 CM SEPARATION
READ PARA TME=200 GEN=160 NPG=1500 NSK=50 NUB=YES
LIB=41 XS1=YES RUN=YES LNG=60000    END PARA
READ MIXT  SCT=3 MIX=1
' U(2.35)02
92400 2.8563-6  92509 3.6755-4  92510 1.2030-4
92600 3.5348-6  92858 2.0009-2  8100 4.1202-2
MIX=2
' water
1102 6.6706-2   8100 3.3353-2
MIX=3
' 6061 Al (clad)
13100 5.8433-2  24100 6.2310-5  29100 6.3731-5
12100 6.6651-4  25100 2.2115-5  22100 2.5375-5
30100 3.0967-5  14100 3.4607-4  26100 1.0152-4
MIX=4
'  1100 Al (top end plug)
13100 5.9660-2  29100 3.0705-5  25100 7.3991-6
30100 1.2433-5  14100 2.3302-4  26100 1.1719-4
MIX=5
' 5052 Al (lower end plug)
13100 5.8028-2  24100 7.7888-5  29100 1.2746-5
12100 1.6663-3  25100 1.4743-5  30100 1.2387-5
14100 1.2978-4  26100 6.5265-5
MIX=6
' acrylic
1102 5.6642-2  6100 3.5648-2  8100 1.4273-2
END MIXT
READ GEOM
UNIT 1
 COM=* FUEL PIN *
 CYLINDER  1 1  0.5588 91.44 0.0
 CYLINDER  4 1  0.5588 91.92 0.0
 CYLINDER  5 1  0.5588 91.92 -1.27
 CYLINDER  3 1  0.635  91.92 -1.27
 CYLINDER  4 1  0.635  96.52 -1.27
 CUBOID  2 1  4P1.016 96.52 -1.27
UNIT 2
 COM=* 20X16 ARRAY OF 320 FUEL PINS *
 ARRAY 1 3R0
UNIT 3
 COM=* 22X16 ARRAY OF 352 FUEL PINS *
 ARRAY 2 3R0
UNIT 4
 COM=* WATER BETWEEN CLUSTERS, 10.05 CM WIDE *
 CUBOID  2 1  10.05 0.0 32.512 0.0 96.52 -1.27
GLOBAL
UNIT 5
 COM=* ARRAY OF 3 CLUSTERS, 1 IN. ACRYLIC BELOW, WATER REFLECTOR *
 ARRAY 3 3R0
 REPLICATE 6 1  5R0.0 2.54  1
 REPLICATE 2 1  4R30.0 9.92 15.3  1
END GEOM
READ ARRAY  ARA=1 NUX=20 NUY=16  FILL F1 END FILL
          ARA=2 NUX=22 NUY=16  FILL F1 END FILL
          ARA=3 NUX=5  FILL 3 4 2 4 3 END FILL
END ARRAY
END DATA
END
```

KENO-V.a Input Listing for Case 1 of Table 14 (27-Energy-Group SCALE4 Cross Sections).

```
=CSAS25
C01  20X18.08 CLUSTER (20X18 + 1 ROD), 2.032 PITCH
27GROUPNDF4 LATTICECELL
' U(2.35)02
U-234  1 0  2.8563-6 295 END
U-235  1 0  4.8785-4 295 END
U-236  1 0  3.5348-6 295 END
U-238  1 0  2.0009-2 295 END
O  1 0  4.1202-2 295 END
' water
H  2 0  6.6706-2 295 END
O  2 0  3.3353-2 295 END
' 6061 Al (clad)
AL  3 0  5.8433-2 295 END
CR  3 0  6.2310-5 295 END
CU  3 0  6.3731-5 295 END
MG  3 0  6.6651-4 295 END
MN  3 0  2.2115-5 295 END
TI  3 0  2.5375-5 295 END
'       (Zn replaced by Cu)
CU  3 0  3.0967-5 295 END
SI  3 0  3.4607-4 295 END
FE  3 0  1.0152-4 295 END
'  1100 Al (top end plug)
AL  4 0  5.9660-2 295 END
CU  4 0  3.0705-5 295 END
MN  4 0  7.3991-6 295 END
'       (Zn replaced by Cu)
CU  4 0  1.2433-5 295 END
SI  4 0  2.3302-4 295 END
FE  4 0  1.1719-4 295 END
' 5052 Al (lower end plug)
AL  5 0  5.8028-2 295 END
CR  5 0  7.7888-5 295 END
CU  5 0  1.2746-5 295 END
MG  5 0  1.6663-3 295 END
MN  5 0  1.4743-5 295 END
'       (Zn replaced by Cu)
CU  5 0  1.2387-5 295 END
SI  5 0  1.2978-4 295 END
FE  5 0  6.5265-5 295 END
' acrylic
H   6 0  5.6642-2 295 END
C   6 0  3.5648-2 295 END
O   6 0  1.4273-2 295 END
' water
H  7 0  6.6706-2 295 END
O  7 0  3.3353-2 295 END
END COMP
SQUAREPITCH 2.032 1.1176 1 2 1.27 3 END
C01  20X18.08 CLUSTER (20X18 + 1 ROD), 2.032 PITCH
READ PARA TME=200 GEN=200 NPG=2000 NSK=50 NUB=YES XS1=YES RUN=YES
END PARA
READ GEOM
UNIT 1
 COM=* FUEL PIN *
 CYLINDER  1 1  0.5588 91.44 0.0
 CYLINDER  4 1  0.5588 91.92 0.0
 CYLINDER  5 1  0.5588 91.92 -1.27
 CYLINDER  3 1  0.635  91.92 -1.27
```

KENO-V.a Input Listing for Case 1 of Table 14 (27-Energy-Group SCALE4 Cross Sections) (cont'd).

```
 CYLINDER  4 1  0.635  96.52 -1.27
 CUBOID  2 1  4P1.016 96.52 -1.27
UNIT 2
 COM=* WATER FUEL PIN *
 CUBOID  7 1  4P1.016 96.52 -1.27
UNIT 3
 COM=* 20X18 ARRAY OF FUEL PINS *
 ARRAY 1 3R0
UNIT 4
 COM=* ONE FUEL PIN AT END OF SIDE *
 ARRAY 2 3R0
GLOBAL
UNIT 5
 COM=* 20X18 ARRAY WITH ONE FUEL PIN ADDED AT END OF SIDE *
 ARRAY 3 3R0
 REPLICATE 6 1  5R0.0 2.54  1
 REPLICATE 7 1  4R30.0 9.92 15.3  1
END GEOM
READ ARRAY  ARA=1 NUX=20 NUY=18  FILL F1 END FILL
         ARA=2 NUX=20 NUY=1  FILL  1 19R2  END FILL
         ARA=3 NUX=1 NUY=2  FILL  3 4  END FILL
END ARRAY
END DATA
END
```

KENO-V.a Input Listing for Case 2 of Table 14 (27-Energy-Group SCALE4 Cross Sections).

```
=CSAS25
C02  CASE 2  THREE 20X17 CLUSTERS, 11.92 CM SEPARATION
27GROUPNDF4 LATTICECELL
' U(2.35)02
U-234  1 0  2.8563-6 295 END
U-235  1 0  4.8785-4 295 END
U-236  1 0  3.5348-6 295 END
U-238  1 0  2.0009-2 295 END
O  1 0  4.1202-2 295 END
' water
H  2 0  6.6706-2 295 END
O  2 0  3.3353-2 295 END
' 6061 Al (clad)
AL  3 0  5.8433-2 295 END
CR  3 0  6.2310-5 295 END
CU  3 0  6.3731-5 295 END
MG  3 0  6.6651-4 295 END
MN  3 0  2.2115-5 295 END
TI  3 0  2.5375-5 295 END
'       (Zn replaced by Cu)
CU  3 0  3.0967-5 295 END
SI  3 0  3.4607-4 295 END
FE  3 0  1.0152-4 295 END
'  1100 Al (top end plug)
AL  4 0  5.9660-2 295 END
CU  4 0  3.0705-5 295 END
MN  4 0  7.3991-6 295 END
'       (Zn replaced by Cu)
CU  4 0  1.2433-5 295 END
SI  4 0  2.3302-4 295 END
FE  4 0  1.1719-4 295 END
' 5052 Al (lower end plug)
AL  5 0  5.8028-2 295 END
CR  5 0  7.7888-5 295 END
CU  5 0  1.2746-5 295 END
MG  5 0  1.6663-3 295 END
MN  5 0  1.4743-5 295 END
'       (Zn replaced by Cu)
CU  5 0  1.2387-5 295 END
SI  5 0  1.2978-4 295 END
FE  5 0  6.5265-5 295 END
' acrylic
H   6 0  5.6642-2 295 END
C   6 0  3.5648-2 295 END
O   6 0  1.4273-2 295 END
' water
H  7 0  6.6706-2 295 END
O  7 0  3.3353-2 295 END
END COMP
SQUAREPITCH 2.032 1.1176 1 2 1.27 3 END
C02  CASE 2  THREE 20X17 CLUSTERS, 11.92 CM SEPARATION
READ PARA TME=200 GEN=160 NPG=1500 NSK=50 NUB=YES XS1=YES RUN=YES
END PARA
READ GEOM
UNIT 1
 COM=* FUEL PIN *
 CYLINDER  1 1  0.5588 91.44 0.0
 CYLINDER  4 1  0.5588 91.92 0.0
 CYLINDER  5 1  0.5588 91.92 -1.27
```

KENO-V.a Input Listing for Case 2 of Table 14 (27-Energy-Group SCALE4 Cross Sections) (cont'd).

```
 CYLINDER  3 1  0.635  91.92 -1.27
 CYLINDER  4 1  0.635  96.52 -1.27
 CUBOID  2 1  4P1.016 96.52 -1.27
UNIT 2
 COM=* 20X17 ARRAY OF 340 FUEL PINS *
 ARRAY 1 3R0
UNIT 3
 COM=* WATER BETWEEN CLUSTERS, 11.92 CM WIDE *
 CUBOID  7 1  11.92 0.0 34.544 0.0 96.52 -1.27
GLOBAL
UNIT 4
 COM=* ARRAY OF 3 CLUSTERS, 1 IN. ACRYLIC BELOW, WATER REFLECTOR *
 ARRAY 2 3R0
 REPLICATE 6 1  5R0.0 2.54  1
 REPLICATE 7 1  4R30.0 9.92 15.3  1
END GEOM
READ PLOT
  XUL=-3 YUL=1.016 ZUL=100 XLR=2.032 YLR=1.016
  ZLR=-5  UAX=1  WDN=-1 NAX=30 NDN=110 NCH=' *~ctla~' END
  XUL=-5 YUL=15 ZUL=2 XLR=15 YLR=-5
  ZLR=2   UAX=1  VDN=-1 NAX=120 NCH=' *~ctla~' END
  XUL=-5 YUL=1.016 ZUL=100 XLR=150 YLR=1.016
  ZLR=-6   UAX=1  WDN=-1 NAX=120 NCH=' *~ctla~' END
  PIC=UNIT XUL=-5 YUL=40 ZUL=2 XLR=150 YLR=-5
  ZLR=2   UAX=1  VDN=-1 NAX=120 NCH=' 12345' END
END PLOT
READ ARRAY  ARA=1 NUX=20 NUY=17  FILL F1 END FILL
          ARA=2 NUX=5  FILL 2 3 2 3 2 END FILL
END ARRAY
END DATA
END
```

KENO-V.a Input Listing for Case 4 of Table 14 (27-Energy-Group SCALE4 Cross Sections).

```
=CSAS25
C04  CASE 4  CENTER 20X16 CLUSTER, TWO 22X16 CLUSTERS, 10.05 CM SEPARATION
27GROUPNDF4 LATTICECELL
' U(2.35)02
U-234  1 0  2.8563-6 295 END
U-235  1 0  4.8785-4 295 END
U-236  1 0  3.5348-6 295 END
U-238  1 0  2.0009-2 295 END
O  1 0  4.1202-2 295 END
' water
H  2 0  6.6706-2 295 END
O  2 0  3.3353-2 295 END
' 6061 Al (clad)
AL  3 0  5.8433-2 295 END
CR  3 0  6.2310-5 295 END
CU  3 0  6.3731-5 295 END
MG  3 0  6.6651-4 295 END
MN  3 0  2.2115-5 295 END
TI  3 0  2.5375-5 295 END
'       (Zn replaced by Cu)
CU  3 0  3.0967-5 295 END
SI  3 0  3.4607-4 295 END
FE  3 0  1.0152-4 295 END
'  1100 Al (top end plug)
AL  4 0  5.9660-2 295 END
CU  4 0  3.0705-5 295 END
MN  4 0  7.3991-6 295 END
'       (Zn replaced by Cu)
CU  4 0  1.2433-5 295 END
SI  4 0  2.3302-4 295 END
FE  4 0  1.1719-4 295 END
' 5052 Al (lower end plug)
AL  5 0  5.8028-2 295 END
CR  5 0  7.7888-5 295 END
CU  5 0  1.2746-5 295 END
MG  5 0  1.6663-3 295 END
MN  5 0  1.4743-5 295 END
'       (Zn replaced by Cu)
CU  5 0  1.2387-5 295 END
SI  5 0  1.2978-4 295 END
FE  5 0  6.5265-5 295 END
' acrylic
H   6 0  5.6642-2 295 END
C   6 0  3.5648-2 295 END
O   6 0  1.4273-2 295 END
' water
H  7 0  6.6706-2 295 END
O  7 0  3.3353-2 295 END
END COMP
SQUAREPITCH 2.032 1.1176 1 2 1.27 3 END
C04  CASE 4  CENTER 20X16 CLUSTER, TWO 22X16 CLUSTERS, 10.05 CM SEPARATION
READ PARA TME=200 GEN=160 NPG=1500 NSK=50 NUB=YES XS1=YES RUN=YES
END PARA
READ GEOM
UNIT 1
 COM=* FUEL PIN *
 CYLINDER  1 1  0.5588 91.44 0.0
 CYLINDER  4 1  0.5588 91.92 0.0
 CYLINDER  5 1  0.5588 91.92 -1.27
```

KENO-V.a Input Listing for Case 4 of Table 14 (27-Energy-Group SCALE4 Cross Sections) (cont'd).

```
 CYLINDER  3 1  0.635  91.92 -1.27
 CYLINDER  4 1  0.635  96.52 -1.27
 CUBOID  2 1  4P1.016 96.52 -1.27
UNIT 2
 COM=* 20X16 ARRAY OF 320 FUEL PINS *
 ARRAY 1 3R0
UNIT 3
 COM=* 22X16 ARRAY OF 352 FUEL PINS *
 ARRAY 2 3R0
UNIT 4
 COM=* WATER BETWEEN CLUSTERS, 10.05 CM WIDE *
 CUBOID  7 1  10.05 0.0 32.512 0.0 96.52 -1.27
GLOBAL
UNIT 5
 COM=* ARRAY OF 3 CLUSTERS, 1 IN. ACRYLIC BELOW, WATER REFLECTOR *
 ARRAY 3 3R0
 REPLICATE 6 1  5R0.0 2.54  1
 REPLICATE 7 1  4R30.0 9.92 15.3  1
END GEOM
READ PLOT
  XUL=-3 YUL=1.016 ZUL=100 XLR=2.032 YLR=1.016
  ZLR=-5  UAX=1  WDN=-1 NAX=30 NDN=110 NCH=' *~ctla~' END
  XUL=-5 YUL=15 ZUL=2 XLR=15 YLR=-5
  ZLR=2   UAX=1  VDN=-1 NAX=120 NCH=' *~ctla~' END
  XUL=-5 YUL=1.016 ZUL=100 XLR=150 YLR=1.016
  ZLR=-6   UAX=1  WDN=-1 NAX=120 NCH=' *~ctla~' END
  PIC=UNIT XUL=-5 YUL=40 ZUL=2 XLR=150 YLR=-5
  ZLR=2   UAX=1  VDN=-1 NAX=120 NCH=' 12345' END
END PLOT
READ ARRAY  ARA=1 NUX=20 NUY=16  FILL F1 END FILL
          ARA=2 NUX=22 NUY=16  FILL F1 END FILL
          ARA=3 NUX=5  FILL 3 4 2 4 3 END FILL
END ARRAY
END DATA
END
```

A.2 MCNP Input Listings

Version 4XD of MCNP was used.

Fuel rod clusters were created by filling cuboids with a universe containing an infinite lattice of fuel rods.

MCNP k_{eff} calculations used 110 generations of 1500 neutrons each after skipping 50 generations.

MCNP Input Listing for Case 1 of Table 14.

```
M01  20X18 +1 CLUSTER OF U(2.35)O2 RODS
1     1 .06170524 -1 7 -8 u=1 imp:n=1 $ uo2 fuel
2     3 .0597516   1 -2 -9 u=1 imp:n=1 $ clad
3     4 .06006075  -1 8 -9 u=1 imp:n=1 $ top end plug (lower piece)
4     4 .06006075  -2 9 u=1 imp:n=1 $ top end plug (top piece)
5     5 .06000711  -1 -7 u=1 imp:n=1 $ lower end plug
6     2 .100059  2 u=1 imp:n=1 $ water
7     0  -4 3 -6 5  imp:n=1 lat=1 u=2 fill=1  $ lattice of fuel rods
8     0 -10 11 -20 21 -22 23 fill=2 imp:n=1  $ rod cluster
9     0  11 -10 19 -21 23 -22  imp:n=1 fill=1  $ one fuel rod
10    6 .106563  19 -20 11 -10 -23 29  imp:n=1  $ acrylic support plate
11    2 .100059 (-11:10:20:-19:22:-29) -24 25 -26 27 -28 30 imp:n=1 $ water
12    0  24:-25:26:-27:28:-30  imp:n=0

1     c/z 1.016 1.016 .5588  $ fuel cylinder
2     c/z 1.016 1.016 .635  $ clad cylinder
3     px  0.0  $ fuel rod cell boundary
4     px  2.032  $ fuel rod cell boundary
5     py  0.0  $ fuel rod cell boundary
6     py  2.032  $ fuel rod cell boundary
7     pz  0.0  $ bottom of fuel
8     pz  91.44  $ top of fuel
9     pz  91.92  $ top of clad
10    px  40.639  $ farthest edge of closest cluster
11    px  .0001  $ closest edge of closest cluster
19    py  0.0001  $ close edge of cluster + one rod
20    py  38.6079  $ sides of clusters
21    py  2.0321  $ side of cluster
22    pz  96.52  $ top of fuel rod
23    pz  -1.27  $ bottom of fuel rod
24    px  70.64  $ side of water reflector
25    px  -30  $ side of water reflector
26    py  68.608  $ side of water reflector
27    py  -30  $ side of water reflector
28    pz  106.44  $ top of water
29    pz  -3.81  $ bottom of acrylic support plate
30    pz  -19.11  $ bottom of water

kcode  1500 1 50 160 50000
sdef  x=d1 y=d2 z=d3 cel=d4
si1   0 41
sp1   0 1
si2   0 37
sp2   0 1
si3   0 92
sp3   0 1
si4   l 8
sp4   v
print
c     m1 is UO2 fuel
m1    92234.50c 2.8563e-6 92235.50c 4.8785e-4
      92236.50c 3.5348e-6 92238.50c 2.0009e-2
      8016.50c  4.1202e-2
c     m2 is water
m2    8016.50c 3.3353e-2  1001.50c 6.6706e-2
mt2   lwtr.01t
c     m3 is 6061 Al (clad)
m3    13027.50c  5.8433e-2  24000.50c  6.2310e-5
      29000.50c  6.3731e-5  12000.50c  6.6651e-4
      25055.50c  2.2115e-5  22000.50c  2.5375e-5
c     Zn replaced by Cu, below
      29000.50c  3.0967e-5  14000.50c  3.4607e-4
```

MCNP Input Listing for Case 1 of Table 14 (cont'd).

```
     26000.50c  1.0152e-4
c    m4 is 1100 aluminum (top end plug)
m4   13027.50c  5.9660e-2  29000.50c  3.0705e-5
     25055.50c  7.3991e-6
c      Zn replaced by Cu, below
     29000.50c  1.2433e-5  14000.50c  2.3302e-4
     26000.50c  1.1719e-4
c    m5 is 5052 aluminum (lower end plug)
m5   13027.50c  5.8028e-2  24000.50c  7.7888e-5
     29000.50c  1.2746e-5  12000.50c  1.6663e-3
     25055.50c  1.4743e-5
c      Zn replaced by Cu, below
     29000.50c  1.2387e-5  14000.50c  1.2978e-4
     26000.50c  6.5265e-5
c    m6 is acrylic (support plate)
m6    1001.50c 5.6642e-2  6000.50c 3.5648e-2
     8016.50c 1.4273e-2
mt6   poly.01t
```

MCNP Input Listing for Case 2 of Table 14.

```
M02  THREE 20X17 CLUSTERS OF U(2.35)O2 RODS, 11.92 CM SEPR, PITCH 2.032 CM
1     1 .06170524 -1 7 -8 u=1 imp:n=1 $ uo2 fuel
2     3 .0597516   1 -2 -9 u=1 imp:n=1 $ clad
3     4 .06006075  -1 8 -9 u=1 imp:n=1 $ top end plug (lower piece)
4     4 .06006075  -2 9 u=1 imp:n=1 $ top end plug (top piece)
5     5 .06000711  -1 -7 u=1 imp:n=1 $ lower end plug
6     2 .100059  2 u=1 imp:n=1 $ water
7     0  -4 3 -6 5  imp:n=1 lat=1 u=2 fill=1  $ lattice of fuel rods
8     0 -10 11 -20 21 -22 23 fill=2 imp:n=1  $ first rod cluster
9     0 -13 12 -20 21 -22 23 fill=2(52.56 0 0) imp:n=1  $ second rod cluster
10    0 -15 14 -20 21 -22 23 fill=2(105.12 0 0) imp:n=1  $ third rod cluster
11    6 .106563  -23 29 -15 11 -20 21 imp:n=1  $ acrylic support plate
12    2 .100059 -12 10 -20 21 -22 23 imp:n=1  $ water between clusters
13    2 .100059 -14 13 -20 21 -22 23 imp:n=1  $ water between clusters
14    2 .100059 (-11:15:20:-21:22:-29) -24 25 -26 27 -28 30 imp:n=1 $ water
15    0  24:-25:26:-27:28:-30  imp:n=0

1     c/z 1.016 1.016 .5588  $ fuel cylinder
2     c/z 1.016 1.016 .635  $ clad cylinder
3     px  0.0  $ fuel rod cell boundary
4     px  2.032  $ fuel rod cell boundary
5     py  0.0  $ fuel rod cell boundary
6     py  2.032  $ fuel rod cell boundary
7     pz  0.0  $ bottom of fuel
8     pz  91.44  $ top of fuel
9     pz  91.92  $ top of clad
10    px  40.639  $ farthest edge of closest cluster
11    px  .0001  $ closest edge of closest cluster
12    px  52.5601  $ closest edge of center cluster
13    px  93.1999  $ farthest edge of center cluster
14    px  105.1201  $ closest edge of farthest cluster
15    px  145.7599  $ farthest end of clusters
20    py  34.54399  $ sides of clusters
21    py  .0001  $ sides of clusters
22    pz  96.52  $ top of fuel rod
23    pz  -1.27  $ bottom of fuel rod
24    px  175.76  $ side of water reflector
25    px  -30  $ side of water reflector
26    py  64.544  $ side of water reflector
27    py  -30  $ side of water reflector
28    pz  106.44  $ top of water
29    pz  -3.81  $ bottom of acrylic support plate
30    pz  -19.11  $ bottom of water

kcode  1500 1 50 160 50000
c     kcode  100 1 1 5 50000
sdef  x=d1 y=d2 z=d3 cel=d4
si1   0 150
sp1   0 1
si2   0 100
sp2   0 1
si3   0 100
sp3   0 1
si4   l 8 9 10
sp4   v
print
c     m1 is UO2 fuel
m1    92234.50c 2.8563e-6 92235.50c 4.8785e-4
      92236.50c 3.5348e-6 92238.50c 2.0009e-2
      8016.50c  4.1202e-2
c     m2 is water
m2    8016.50c 3.3353e-2  1001.50c 6.6706e-2
```

MCNP Input Listing for Case 2 of Table 14 (cont'd).

```
mt2   lwtr.01t
c     m3 is 6061 Al (clad)
m3    13027.50c  5.8433e-2  24000.50c  6.2310e-5
      29000.50c  6.3731e-5  12000.50c  6.6651e-4
      25055.50c  2.2115e-5  22000.50c  2.5375e-5
c     Zn replaced by Cu, below
      29000.50c  3.0967e-5  14000.50c  3.4607e-4
      26000.50c  1.0152e-4
c     m4 is 1100 aluminum (top end plug)
m4   13027.50c  5.9660e-2  29000.50c  3.0705e-5
      25055.50c  7.3991e-6
c       Zn replaced by Cu, below
      29000.50c  1.2433e-5  14000.50c  2.3302e-4
      26000.50c  1.1719e-4
c     m5 is 5052 aluminum (lower end plug)
m5   13027.50c  5.8028e-2  24000.50c  7.7888e-5
      29000.50c  1.2746e-5  12000.50c  1.6663e-3
      25055.50c  1.4743e-5
c       Zn replaced by Cu, below
      29000.50c  1.2387e-5  14000.50c  1.2978e-4
      26000.50c  6.5265e-5
c     m6 is acrylic (support plate)
m6    1001.50c 5.6642e-2  6000.50c 3.5648e-2
      8016.50c 1.4273e-2
mt6   poly.01t
```

MCNP Input Listing for Case 4 of Table 14.

```
M04  TWO 22X16 CLUSTERS, ONE 20x16, OF U(2.35)O2 RODS, 10.05 CM SEPR
1     1 .06170524 -1 7 -8 u=1 imp:n=1 $ uo2 fuel
2     3 .0597516   1 -2 -9 u=1 imp:n=1 $ clad
3     4 .06006075  -1 8 -9 u=1 imp:n=1 $ top end plug (lower piece)
4     4 .06006075  -2 9 u=1 imp:n=1 $ top end plug (top piece)
5     5 .06000711  -1 -7 u=1 imp:n=1 $ lower end plug
6     2 .100059  2 u=1 imp:n=1 $ water
7     0  -4 3 -6 5  imp:n=1 lat=1 u=2 fill=1  $ lattice of fuel rods
8     0 -10 11 -20 21 -22 23 fill=2 imp:n=1  $ first rod cluster
9     0 -13 12 -20 21 -22 23 fill=2(54.754 0 0) imp:n=1  $ second rod cluster
10    0 -15 14 -20 21 -22 23 fill=2(105.444 0 0) imp:n=1  $ third rod cluster
11    6 .106563  -23 29 -15 11 -20 21 imp:n=1  $ acrylic support plate
12    2 .100059 -12 10 -20 21 -22 23 imp:n=1  $ water between clusters
13    2 .100059 -14 13 -20 21 -22 23 imp:n=1  $ water between clusters
14    2 .100059 (-11:15:20:-21:22:-29) -24 25 -26 27 -28 30 imp:n=1 $ water
15    0  24:-25:26:-27:28:-30  imp:n=0

1     c/z 1.016 1.016 .5588  $ fuel cylinder
2     c/z 1.016 1.016 .635  $ clad cylinder
3     px  0.0  $ fuel rod cell boundary
4     px  2.032  $ fuel rod cell boundary
5     py  0.0  $ fuel rod cell boundary
6     py  2.032  $ fuel rod cell boundary
7     pz  0.0  $ bottom of fuel
8     pz  91.44  $ top of fuel
9     pz  91.92  $ top of clad
10    px  44.7039  $ farthest edge of closest cluster
11    px  .0001  $ closest edge of closest cluster
12    px  54.7541  $ closest edge of center cluster **
13    px  95.3939  $ farthest edge of center cluster
14    px  105.4441  $ closest edge of farthest cluster **
15    px  150.1479  $ farthest end of clusters
20    py  32.5119  $ sides of clusters
21    py  .0001  $ sides of clusters
22    pz  96.52  $ top of fuel rod
23    pz  -1.27  $ bottom of fuel rod
24    px  180.148  $ side of water reflector
25    px  -30  $ side of water reflector
26    py  62.512  $ side of water reflector
27    py  -30  $ side of water reflector
28    pz  106.44  $ top of water
29    pz  -3.81  $ bottom of acrylic support plate
30    pz  -19.11  $ bottom of water

kcode  1500 1 50 160 50000
c     kcode  100 1 1 5 50000
sdef  x=d1 y=d2 z=d3 cel=d4
si1   0 151
sp1   0 1
si2   0 100
sp2   0 1
si3   0 100
sp3   0 1
si4   l 8 9 10
sp4   v
print
c     m1 is UO2 fuel
m1    92234.50c 2.8563e-6 92235.50c 4.8785e-4
      92236.50c 3.5348e-6 92238.50c 2.0009e-2
      8016.50c  4.1202e-2
c     m2 is water
m2    8016.50c 3.3353e-2  1001.50c 6.6706e-2
```

MCNP Input Listing for Case 4 of Table 14 (cont'd).

```
mt2   lwtr.01t
c     m3 is 6061 Al (clad)
m3    13027.50c  5.8433e-2  24000.50c  6.2310e-5
      29000.50c  6.3731e-5  12000.50c  6.6651e-4
      25055.50c  2.2115e-5  22000.50c  2.5375e-5
c     Zn replaced by Cu, below
      29000.50c  3.0967e-5  14000.50c  3.4607e-4
      26000.50c  1.0152e-4
c     m4 is 1100 aluminum (top end plug)
m4   13027.50c  5.9660e-2  29000.50c  3.0705e-5
      25055.50c  7.3991e-6
c       Zn replaced by Cu, below
      29000.50c  1.2433e-5  14000.50c  2.3302e-4
      26000.50c  1.1719e-4
c     m5 is 5052 aluminum (lower end plug)
m5   13027.50c  5.8028e-2  24000.50c  7.7888e-5
      29000.50c  1.2746e-5  12000.50c  1.6663e-3
      25055.50c  1.4743e-5
c       Zn replaced by Cu, below
      29000.50c  1.2387e-5  14000.50c  1.2978e-4
      26000.50c  6.5265e-5
c     m6 is acrylic (support plate)
m6    1001.50c 5.6642e-2  6000.50c 3.5648e-2
      8016.50c 1.4273e-2
mt6   poly.01t
```

A.3 ONEDANT/TWODANT Input Listings

Because of the heterogeneity of the fuel rod lattice, neither ONEDANT nor TWODANT calculations were performed.

APPENDIX B: CORRELATION BETWEEN CASE NUMBER AND ORIGINAL EXPERIMENT NUMBER

Table B.1 correlates the experiment "Case" number, as used in this evaluation, with the original experiment number. Logbooks are stored at the Los Alamos National Laboratory Archives under the original experiment number. (Logbooks for all experiments below were listed on the inventory for the shipment from Hanford to Los Alamos as being in Box 11.)

Table B.1. Correlation of Case Number with Original Experiment Number.

Case Number	Original Experiment Number
1	SSC-2.35-000-002[(a)]
2	SSC-2.35-000-015[(a)]
3	SSC-2.35-000-005,013,014,049[(a)] SSC-2.35-000-(055-068)
4	SSC-2.35-000-018[(a)]
5	SSC-2.35-000-022[(a)]
6	SSC-2.35-000-045
7	SSC-2.35-000-021[(a)]
8	SSC-2.35-000-(055-068)

(a) Erroneously listed in the "Abbreviated Inventory List for Critical Experiment Data Log Books from Hanford Plutonium Critical Mass Laboratory (Boxes No. 1 through 15)" as SSC-413-000-0XX.

APPENDIX C: EFFECT OF WATER IMPURITIES ON k_{eff}

Results of analyses of water impurities from References 1-10 are given in Table C.1.

Note that two sets of results from Reference 8, the gadolinium-water experiments, are given. Two separate analyses, one of the gadolinium solution and the other of the gadolinium nitrate powder, were done. The first set of values is the largest amount of impurity found in any solution sample used in an approach to critical experiment (Reference 8, p. C.4). The second set of values is from the gadolinium nitrate powder analysis and is based on the highest gadolinium concentration used, which was 1.481 g Gd/liter (0.00148 g Gd/cm^3). Shaded concentrations are maximum values.

Concentrations of impurities in solution from their weight percent in gadolinium nitrate powder were calculated in the following manner: The molecular formula for the gadolinium nitrate powder is given as $Gd(NO_3)_3 \times 4.91\ H_2O$, giving a molecular weight of 431.72. Therefore, assuming a solution concentration of 1.481 g Gd/liter, the concentration of the impurity in solution from the given weight percent of the impurity in the gadolinium nitrate powder (Reference 8, p. C.3) is:

$$0.001481\frac{g}{cm^3}\ \frac{(wt.\%\ impurity)}{(wt.\%\ Gd)} = \frac{.001481\frac{g}{cm^3}(wt.\%\ impurity)}{[100 - \sum(wt.\%\ impurities)]\frac{A_{W,Gd}}{M_{W,Gd\ powder}}}$$

$$= \frac{0.001481\frac{g}{cm^3}(wt.\%\ impurity)}{[100 - 0.4735]\frac{157.25}{431.72}} = 4.08534 \times 10^{-5}(wt.\%\ impurity)\frac{g}{cm^3}$$

Table C.1. Impurity Components of Water (g/m^3).[a] (Maximum values are shaded.)

Reference→ Component↓	1, p. 8[b]	2 (p. 6) and 3 (p. 7)[c]	4 (p. 8)[c]	5 (p. 9); 6 (p. 7); 7 (p. 6)[d]	8 (p. C.4)	8 (p. C.3)	9 (p. B.2)[e]	10 (p. B.2)
Cl	26.2±5.4	30.2±5.8	1.7±.6	≤ 5	-	-	11	18
NO_3^-	0.24±.12	0.42±.16	0.02±.01	0.02	-	-	<0.38[f]	2.83[f]
Cr	<0.028	<0.01	<0.01	<0.01	-	0.041	<0.01	<0.005
Zn	0.35±.05	0.26±.07	0.9±1.1	16	10.6	0.0613	<0.05	0.32
Mn	<0.55	<0.01	<0.01	<0.01	-	0.041	<0.01	<0.01
Pb	<0.015	<0.005	0.008±.001	<0.005	2.1	1.0220	<0.002	<0.005
F	0.21±.02	0.15±.04	0.15±.04	0.18	-	-	0.12	0.12
Fe	<0.06	<0.03	<0.03	24	-	0.21	0.12	0.20
Cu	<0.06	<0.01	<0.01	<0.01	18.2	0.123	<0.05	<0.05
Cd	0.004±.001	0.006±.001	0.020±.006	0.001	-	0.041	0.002	0.0006
Gd	-	-	10.4±3.6	-	-	-	-	<10
SO_3	6.7±.4	6.6±.04	13.4±5.0	14.5	-	-	21	16
$CaCO_3$	-	-	-	-	19.2[g]	1.02[g]	51.2	35
B	-	-	-	-	0.09	1.02	-	<25
Al	-	-	-	-	7.3	2.04	-	-
Eu	-	-	-	-	0.08	1.23	-	-
Mg	-	-	-	-	5.7	0.204	-	-
Nd	-	-	-	-	12.2	2.04	-	-
Si	-	-	-	-	3.1	2.04	-	-
Ni	-	-	-	-	6.8	0.204	-	-
Y	-	-	-	-	0.17	0.41	-	-

Reference→ Component↓	1, p. 8[b]	2 (p. 6) and 3 (p. 7)[c]	4 (p. 8)[c]	5 (p. 9); 6 (p. 7); 7 (p. 6)[d]	8 (p. C.4)	8 (p. C.3)	9 (p. B.2)[e]	10 (p. B.2)
Others	-	-	-	-	Nb 0.3	Ag .041 Au .041 Ba .041 Be 2.04 Ce .102 Co .041 Dy .204 Hf .041 K .204 Li .041 La .204 Mo .041 Na 1.02 Pt .204 Rh .102 Ru 1.02 Sm .204 Sn 1.02 Sr .041 Tb .204 Ti 2.04 U .204 V .041 W .102 Zr .041	-	-
Dissolved Solids (g/m^3)	-	137±5	113±28	61 ± 3	-	-	109	83

(a) If one cubic centimeter has a mass of 1 gram, then this is the same as PPM (parts per million) by weight.
(b) Average of samples taken at the beginning and near the end of the experiments.
(c) Error limits are standard deviations observed in three samples.
(d) In Reference 7, analysis is prior to boron additions (Reference 7, p. 2).
(e) Largest values of three samples.
(f) "Nitrate (as N) mg/liter."
(g) As Ca.

Effect Due to Water Density Reduction - The maximum amount of dissolved solids reported was 137 grams per cubic meter of solution. Assume that the dissolved solids at a concentration of 200 g/m^3, have the same density as water (~1 g/cm^3), and displace the water. These are conservative assumptions since the 200 g/m^3 concentration is greater than any measured total impurity concentration and since many materials are denser than water and, when dissolved in water, do not displace as much water as their dry volume. The percentage of water volume displaced by the solute is then $200/10^6 \times 100 = 0.02\%$. To see the effect of reduced water density, the water volume fraction is reduced by this percentage. The resulting change in k_{eff} of this conservative approximation is is less than 0.04%.[a] Therefore, the effect on k_{eff} of water density reduction due to impurities is negligible.

[a] This is based on ONEDANT calculations of $U(2.35)O_2$ fuel rods in a cylindrical, water-reflected, near-optimal square-pitched array, using 27-group cross sections created by CSASIX.

Effect Due to Presence of Individual Impurities - Listed in Table C.2 are the percent changes in k_{eff} for the addition of the maximum measured amounts of each impurity, as calculated by ONEDANT, using the 27-group cross sections processed by CSASIX.[a] No changes are greater than 0.005% except those from boron and gadolinium impurities, with Δk_{eff} values of 0.9% and 1.7%, respectively. Therefore, critical configurations from the two references with these maximal possible impurity concentrations, References 4 and 10, should include these two impurities in the water.

Table C.2. Calculated Effect of Impurities on Δk_{eff}.

Impurity	Concentration (g/cm^3)	Atom Density (atoms/barn-cm)	% Δk_{eff}
Ag	4.09×10^{-08}	2.281×10^{-10}	0
Al	7.30×10^{-06}	1.629×10^{-07}	0
Au	4.09×10^{-08}	1.249×10^{-10}	0
B	2.50×10^{-05}	1.393×10^{-06}	-0.885 -0.784(a)
	1.02×10^{-06}(b)	5.682×10^{-08}	-0.009
Ba	4.09×10^{-08}	1.791×10^{-10}	0
Be	2.04×10^{-06}	1.365×10^{-07}	0.002
$CaCO_3$	5.12×10^{-05}	3.081×10^{-07}	0.005
Cd	4.09×10^{-08}	2.189×10^{-10}	0
Ce	1.02×10^{-07}	4.390×10^{-10}	0.001
Cl	3.60×10^{-05}	6.115×10^{-07}	0.004
Co	4.09×10^{-08}	4.175×10^{-10}	0
Cr	4.09×10^{-08}	4.732×10^{-10}	0
Cu	1.82×10^{-05}	1.725×10^{-07}	0.002
Eu	1.22×10^{-06}	4.838×10^{-09}	-0.005
F	2.30×10^{-07}	7.291×10^{-09}	0
Fe	2.40×10^{-05}	2.588×10^{-07}	0.003

[a] Because zinc and platinum were not in the Standard Composition Library for CSAS, copper was substituted for zinc and gold was substituted for platinum. (Copper and gold total cross sections appear to be similar, conservative substitutes for zinc and platinum.)

Impurity	Concentration (g/cm^3)	Atom Density (atoms/barn-cm)	% Δk_{eff}
Gd	1.40×10^{-05}	5.361×10^{-08}	-1.653 -1.830[a]
	1.00×10^{-05}[c]	3.830×10^{-08}	-1.200
	5.00×10^{-06}[d]	1.915×10^{-08}	-0.592
Hf	4.09×10^{-08}	1.378×10^{-10}	0
K	2.04×10^{-07}	3.146×10^{-09}	0
Li	4.09×10^{-08}	3.544×10^{-09}	0
La	2.04×10^{-07}	8.856×10^{-10}	0
Mg	5.70×10^{-06}	1.412×10^{-07}	0
Mn	5.50×10^{-07}	6.029×10^{-09}	0.002
Mo	4.09×10^{-08}	2.564×10^{-10}	0
N	2.83×10^{-06}	1.217×10^{-07}	0.002
Na	1.02×10^{-06}	2.675×10^{-08}	0.002
Nb	3.00×10^{-07}	1.945×10^{-09}	0
Nd	1.22×10^{-05}	5.094×10^{-08}	0.001
Ni	6.80×10^{-06}	6.977×10^{-08}	0.002
Pb	2.10×10^{-06}	6.103×10^{-09}	0
Pt[e]	2.04×10^{-07}	6.305×10^{-10}	0
Rh	1.02×10^{-07}	5.977×10^{-10}	0.001
Ru	1.02×10^{-06}	6.085×10^{-09}	0.001
Si	3.10×10^{-06}	6.647×10^{-08}	0
Sm	2.04×10^{-07}	8.179×10^{-10}	0.001
Sn	1.02×10^{-06}	5.182×10^{-09}	0
SO_3	1.84×10^{-05}	1.384×10^{-07}	0.002
Sr	4.09×10^{-08}	2.808×10^{-10}	0.001
Tb	2.03×10^{-07}	7.709×10^{-10}	0.001
Ti	2.04×10^{-06}	2.568×10^{-08}	0
U	2.04×10^{-07}	5.168×10^{-10}	0
V	4.09×10^{-08}	4.830×10^{-10}	0
W	1.02×10^{-07}	3.345×10^{-10}	0

Impurity	Concentration (g/cm^3)	Atom Density (atoms/barn-cm)	% Δk_{eff}
Y	4.09×10^{-07}	2.767×10^{-09}	0
Zn[(f)]	1.60×10^{-05}	1.474×10^{-07}	0.003
Zr	4.09×10^{-08}	2.697×10^{-10}	0

(a) MCNP calculation.
(b) This is an actual measured value, from Reference 8.
(c) Measured maximum value from Reference 10.
(d) Half of measured maximum value from Reference 10.
(e) Because platinum was not in the cross-section library, gold was substituted.
(f) Because zinc was not in the cross-section library, copper was substituted.

APPENDIX D: SAMPLE CSASIX AND ONEDANT INPUTS FOR SENSITIVITY STUDIES USING HOMOGENIZED FUEL ROD REGION

```
=CSASIX
GENERATE 27-GRP LIB FOR 2.35 WT% UO2 PNL FUEL PINS IN WATER
27GROUPNDF4 LATTICECELL
U-234  1 0  2.85626-6 291 END
U-235  1 0  4.87852-4 291 END
U-236  1 0  3.53484-6 291 END
U-238  1 0  2.00094-2 291 END
O  1 0  4.12021-2 291 END
H  2 0  6.67619-2 291 END
O  2 0  3.33809-2 291 END
Al  3 0  6.01507-2 291 END
H  4 0  6.67619-2 291 END
O  4 0  3.33809-2 291 END
END COMP
SQUAREPITCH 2.032 1.1176 1 2 1.27 3 END
END


    1     0     0
SLAB OF U(2.35)O2 FUEL PINS IN WATER, BASE CASE
/  Block 1
igeom=slab ngroup=27 isn=16 niso=5 mt=5 nzone=5 im=4 it=251  T

/  Block 2
xmesh= 0 44.72 45.72 46.72 60.72
xints= 179    8     8     56
zones=   5    5     4      4 T

/  Block 3
lib=xs27.p3
chivec= .021 .188 .215 .125 .166 .180 .090 .014 .001 18z
maxord=3 ihm=42 iht=3 ihs=16 ititl=1 ifido=2 i2lp1=1
T

/ Block 4
matls=isos  assign=matls  T

/  Block 5
ievt=1 isct=3 ibl=1 ibr=0 epsi=.000001  T

/  Block 6
pted=0 zned=1  T
```